J. Quant. Spectrosc. Radiat. Transfer. Vol. 11, pp. 1401–1439. Pergamon Press 1971. Printed in Great Britain

EXCITATION OF N_2 AND N_2^+ SYSTEMS BY ELECTRONS—II EXCITATION CROSS SECTIONS AND $N_2 1PG$ LOW PRESSURE AFTERGLOW

D. E. SHEMANSKY

Department of Physics, University of Pittsburgh, Penn. 15213, U.S.A.

and

A. L. BROADFOOT

Kitt Peak National Observatory, Tucson, Arizona 85717, U.S.A.

(*Received* 11 *January* 1971)

Abstract—Quantitative optical measurements of the $N_2 1P$, $2P$, and N_2^+ Meinel systems excited by electrons have allowed measurement of transition probabilities, excitation cross-sections, and afterglow effects. The excitation cross-sections were determined relative to that of the $N_2^+(0,0)$ first negative band. The estimated total peak electron cross-section of the $B\,^3\Pi_g$ state is 1.2×10^{-16} cm^2, about a factor of 2 larger than other recently published estimates. The total peak cross-section of the $C\,^3\Pi_u$ state is estimated to be 3.8×10^{-17} cm^2.

The $B\,^3\Pi_g v > 4$ levels are excited by a low-pressure afterglow, as well as by electrons. The characteristics of the afterglow suggest that the precursors must be molecules in the $A\,^3\Sigma_u^+$ state. The rate coefficients for collisional deactivation into the $B\,^3\Pi_g$ state fall in the gas-kinetic range. The afterglow contribution is substantial for some levels; at pressures $>3\,\mu$, 90 per cent of the $B\,^3\Pi_g v = 12$ level population rate is due to deactivation of the $A\,^3\Sigma_u^+$ state.

Measurements of the N_2^+ Meinel system are complicated by what appears to be drift in the electric field caused by differential diffusion of electrons and ions. As a result, collision-free measurements of electron excitation cross-sections were not possible, and the cross-section estimates depend on the value of the natural lifetime of the $A\,^2\Pi_u$ state. However, the lifetime is not well determined and we assign a lower limit estimate to the total cross-section of 1.2×10^{-16} cm^2 at $E = 100$ eV. This estimate is between factors of 2 and 5 larger than earlier published values.

1. INTRODUCTION

THE N_2 first positive ($1P$), second positive ($2P$), and N_2^+ Meinel (M) systems, well known in both aeronomy and the laboratory, have been the subjects of a number of recent publications concerned with optical-electron gun measurements of excitation cross-sections.[1–8]

The results for the $N_2 1PG$ ($B\,^3\Pi_g - A\,^3\Sigma_u^+$), Refs. (1, 2, 7, 8) do not correlate satisfactorily. The relative population rates of the $B\,^3\Pi_g$ levels obtained from the first two sets of measurements do not agree. Consequently, the cross-section measurements of the two groups agree or disagree depending on the vibrational levels chosen for comparison. Only the total cross-section of the $B\,^3\Pi_g$ state has been made available from the work of Refs. (7, 8). The peak cross-section given in the two publications by the same authors differ by a factor of 1.4, and are between factors of 1.5 and 2.5 larger than the results of Refs. (1 and 2). There is good agreement, in general, on the shapes of the excitation functions at low electron energies with some differences in detail. We regard the higher energy cross-sections of both

the $B\,^3\Pi_g$ and $C\,^3\Pi_u$ states as untrustworthy due to possible excitation by reflected or scattered electrons.

Measurements of the excitation function of the $N_2 2PG$ (0, 0) ($C\,^3\Pi_u - B\,^3\Pi_g$) band at low energies are in good agreement (cf. (5)) with one exception; the results of Refs. (7, 8), as communicated by Ref. (5), are about a factor of 1.5 lower in magnitude than the remaining work. Although the Ref. (5 and 6) measurements are in good agreement on the cross-section of the (0, 0) band, there is disagreement on the total cross-section of the $C\,^3\Pi_u$ state. The evidence indicates the Ref. (6) measurements are probably in error, since their results do not correspond well with the apparently well established transition probabilities of the $C\,^3\Pi_u - B\,^3\Pi_g$ system.

The measurements of the $N_2^+ M(A\,^2\Pi_u - X\,^2\Sigma_g^+)$ system[2,3,4,7,8] have produced complete confusion. Estimates of the excitation cross-sections of the $A\,^2\Pi_u$ state differ by an order of magnitude. The shape of the excitation function has not been established, and measurements of relative population rates are in disagreement.

The analyses of recent observations of the systems are presented here which we believe may indicate the sources of most of the discrepancies among the previously published work. The results of the present observations differ substantially with the earlier articles on the $N_2 1P$ and $N_2^+ M$ systems. The origin of the disagreement appears to be due to instrumental calibration only to a relatively minor degree. According to our interpretation of the evidence, the excitation of both systems for the purpose of cross-section measurement is somewhat more complicated than has been implied in the recent literature. We suggest in the following discussion that the work of Refs. (1–4, 7, 8), is probably in error, partly because the comparatively long lifetimes of these two systems have apparently been ignored and partly because the $N_2 1PG$ is affected by a low-pressure afterglow.

The lifetimes of the $N_2 1PG$ have been well established by the measurements of JEUNEHOMME[9] and others (cf. Part I; Ref. 10), at values in the region between 9 and 4 μsec, depending on the vibrational level. In most experimental arrangements, the excited molecules ($B\,^3\Pi_g$) would diffuse out of the electron beam, creating a condition in which the volume-production rate is measureably different from the volume-emission rate. If the instrumental field-of-view is restricted to accommodate only the size of the beam, the estimates of excitation cross-sections must then be made through knowledge of the natural lifetime. Preferably, the optical geometry should be arranged so that in effect one measures the volume production rate directly (cf. Part I). The magnitude of the lifetime in relation to the width of the electron beam, in this case, is an important consideration that has not been discussed in any of the preceding articles. Thus we have the possibility that the cross-sections could be under-estimated. This point is raised here since it appears to be the most plausible reason for the $B\,^3\Pi_g v < 5$ cross-sections obtained in the present work, to be larger than those of Refs. (1 and 2). The present total peak cross-section of the $B\,^3\Pi_g$ state ($QB = 1.2 \times 10^{-16}$ cm^2) is about a factor of 2 greater than the latter work. Part of this factor is due to inaccurate transition probabilities (cf. Part I). An additional contribution in the other direction due to the afterglow will be discussed below. After taking these factors into account, there remains a discrepancy of roughly 1.5, which is explained most plausibly as a consequence of diffusion of the $B\,^3\Pi_g$ molecules. References (7 and 8) give peak values $QB = 1.4 \times 10^{-16}$ cm^2 and 1.0×10^{-16} cm^2, respectively. The rough agreement with the present work cannot be taken too seriously due to unknown contributions from the first two sources of discrepancy mentioned above.

A clear warning that the $N_2 1PG$ excited by low energy electrons at low pressures may be affected by an afterglow process arises in the early careful work of THOMPSON and WILLIAMS.[11] A diffuse glow surrounding the electron beam at energies above 10.5 eV (pressure $P \approx 3\,\mu$) was shown to be due to $N_2 1PG$ bands. The glow differed from the Lewis–Rayleigh (L–R) afterglow in that all levels were well represented from $v' = 12$ down. The glow was somewhat more extensive than one might expect from the presently known lifetime, and OLDENBERG[12] suggested that it may be due to the diffusion of $a\,^1\Pi_g$ molecules with subsequent collision transfer to the $B\,^3\Pi_g$ state. We now know that this could not be the case since the threshold energy for the process is too low to be consistent with the production of significant quantities of $a^1\Pi_g$ molecules. The more recent low-pressure lifetime measurements by Jeunehomme, which indicated significant contributions from other long-lived sources, are interpreted here as further evidence for the presence of an afterglow. The present observations of the $N_2 1P$ system described below show the distinct presence of an afterglow affecting the $v' = 5$ to 12 levels at pressures down to $P = 0.5\,\mu$. The nature of the afterglow suggests strongly that the precursors are molecules in the $A\,^3\Sigma_u^+$ state. The presence of the afterglow would be very difficult to avoid in any experimental arrangement and must be present in varying degrees in all of the electron-gun experiments. However, the afterglow could easily go unrecognized since it is very nearly first order in $[N_2]$ at all but the lowest pressures. In the discussion that follows it will be shown that the previous electron cross-section estimates for the higher vibrational levels very likely are in error due to significant afterglow contributions. The afterglow, to which we apply the term 'degenerate L–R afterglow', will be discussed quantitatively in terms of the probable relationship to the L–R afterglow observed at pressures $> 100\,\mu$.

The much shorter lifetime of the $C\,^3\Pi_u$ state simplifies cross-section measurements of the $N_2 2PG$ ($C\,^3\Pi_u - B\,^3\Pi_g$). The peak cross-section of the $N_2 2P(0,0)$ band given by the present work (1.04×10^{-17} cm^2) is in good agreement with the measurements of Refs. (5, 6). The excitation function has been determined at low electron energies only, since unknown contributions due to re-excitation by secondary electrons appear to affect the measurements at high energies. A compilation of measurements in the literature indicates that the relative population rates of the $C\,^3\Pi_u$ state follow the Franck–Condon factors for the ($C\,^3\Pi_u - X\,^1\Sigma_g^+$) transition. The results presented by Ref. (6) are at variance, but as we imply above this reduces to a question of whether the $N_2 2PG$ transition probabilities are correct. The transition probabilities appear to be well established, and those measurements which are in good agreement with the Wallace and Nicholls–Tyte values for the ($C\,^3\Pi_u - B\,^3\Pi_g$) transition also give relative population rates ($C\,^3\Pi_u - X\,^1\Sigma_g^+$) close to the theoretical values. The present estimate of the total peak cross-section is $QC = 3.8 \times 10^{-17}$ cm^2.

A certain risk accompanies the application of direct proportionality of emission rate with pressure and electron current as the sole criterion for determining the absence of secondary processes, since the possibility of a first order dependence over large regions of pressure and current is excluded. As we have indicated this appears to have led to large errors in the cross-sections of the high levels of the $B\,^3\Pi_g$ state, due to contributions from the afterglow. The earlier measurements of the $N_2^+ M$ cross-sections,[3,4,7,8] according to the present analysis, are probably in error for a similar reason. The present observations of lifetime as a function of pressure and current, and Stern–Volmer plots obtained from steady state measurements, are consistent with a relatively large radiationless deactivation

rate at low pressure as a result of diffusion or drift in an electric field. The electric field, arising in the differential diffusion rates of the secondary electrons and the N_2^+ ions is pressure, energy, and current dependent in a very ill defined relationship. The estimation of the excitation cross-section in the present work thus depends on knowledge of the natural lifetime. The extrapolation of the natural lifetime to zero pressure can be relied upon only as a measure of a lower limit to the real value. The only other measurements of $A\,^2\Pi_u$ lifetime in the literature are those of SHERIDAN *et al.*,[13] O'NEIL and DAVIDSON[14] and HOLLSTEIN *et al.*[15] Reference (13) gave only a very rough estimate (3 μsec) based on the spreading of the emission from the electron beam. The measurements of Ref. (14) have similar characteristics to the present work but result in longer lifetimes, 6.8 μsec compared to 4.4 μsec for the $A\,^2\Pi_u v = 2$ level. The Ref. 14 estimates have been adopted in the present determination of the excitation cross-sections. The cross-section at 100 eV on this basis is 1.2×10^{-16} cm^2, as a lower limit estimate. The lifetime measurements of Ref. (15) (12 μsec) are too large to be compatible with the present observations; the resulting cross-section would be equal to the well established total ionization cross-section. The variability in the shapes of the published excitation functions[4] may well originate with the electron energy and current dependence of the diffusion rate. The uncorrected excitation functions of the present work in fact display shapes similar to all of those in the literature. The shape of the excitation function, corrected for the variable diffusion rate with the aid of lifetime measurements, has been determined up to ($E =$) 100 eV. The function is linear in E up to about 30 eV, with a peak in the region of 100 eV. This is compatible with the threshold measurements of total ionization cross-sections of N_2,[16,17] which is also linear between 19 eV and 30 eV. The slope of the excitation function of the $A\,^2\Pi_u$ state determined from the total ionization measurements near threshold yields a value in good agreement with the slope (cm^2/eV) obtained from the present measurements. The cross-section given here indicates that at least 60 per cent of the total ionization of N_2 goes into the $A\,^2\Pi_u$ state. This result is consistent with photoionization measurements by SCHOEN.[18]

2. EXPERIMENTAL

Details of the experimental arrangement are given in Part I. The measurements were all made in pure research grade N_2. Pulse counting techniques were used for all of the measurements. The spectra were obtained with 1 m and $\frac{1}{2}$ m Ebert–Fastie type scanning spectrometers, operated in the 1st order to observe the $N_2 1P$ and $N_2^+ M$ systems in the 5000–10,650 Å region ($\Delta\lambda = 10$ Å) and in the second order ($\Delta\lambda = 5$ Å) to observe the N_2^+ first negative ($1N$) and $N_2 2P$ systems. The observations were recorded in single long scans. Fluctuations in excitation rate as a function of scan time were compensated for by controlling the stepping rate of one spectrometer with the signal from the other. The control spectrometer monitored either the $N_2^+ 1N(0,0)$, $N_2 1P(6,3)$, or $N_2 2P(0,0)$ bands. Calibration of the instrumental spectral sensitivity is discussed in Part I. The relative intensities of the $N_2 1P$ and $N_2^+ M$ bands were determined by comparison with accurate synthetic spectra (Refs. 19, 20, cf. Part I), in order to reduce errors due to overlapping emission from other bands and atomic lines.

Accurate relative vibrational population rates and hence cross-sections depend on the determination of accurate transition probabilities for the entire band system. Improved

transition probabilities were judged necessary for the $N_2 1P$ and $N_2^+ M$ systems. Tables for the two systems have been calculated from the present measurements and are given in Part I, along with values for the $N_2 2P$ and $N_2^+ 1N$ systems compiled from earlier work. The relative population rates and cross-sections given in this article are based on these tables.

Cross-sections have been determined by measuring one or two bands of each system relative to the $N_2^+ 1N(0, 0)$ band. Total system cross-sections were then calculated using the estimated relative population rates. This technique required an accurate measure of the shape of the $N_2^+ 1N$ excitation function from threshold, since the cross-sections of the N_2 positive systems at low electron energies are of considerable importance. The measured $N_2^+ 1N$ excitation function has a linear dependence on E from threshold to about 30 eV and agrees closely with the shape given by Zipf and Borst.[21] The cross-section measurements of Ref. (21) for the $N_2^+ 1N(0, 0)$ band have therefore been adopted here.

The approach to the measurement of the excitation cross-section of the $N_2 2P$ system was straightforward since the lifetime of the $C\,^3\Pi_u$ state is short, 4.5×10^{-8} sec (Ref. 22, cf. 23). The (0, 2) band was compared simultaneously with the $N_2^+ 1N$ (0, 0) band at electron energies down to $E = 22$ eV. The observations were made at collision-free pressures for the $C\,^3\Pi_u$ state and at beam currents in the region where proportionality with intensity was obtained. The $N_2 2PG$ cross-section estimate of the present work stems from the measurement of this single band. The validity of the transition probabilities and relative population rates used for the calculation are discussed in detail in Part I and Section IV.

The measurement of the $N_2 1P$ and $N_2^+ M$ systems required a different approach since the lifetimes of both are much longer, in the region of 10^{-5} sec, and were subject to radiationless deactivation with essentially unknown rate coefficients. The technique in this case was to measure lifetime and intensity at the same time using the same beam current for both measurements. This has the advantage of providing a much greater sensitivity for the detection of secondary processes, than the common method in which one relies solely on steady state measurements. The lifetime measurements were made by gating the electron beam with a 10 kc square wave, and also with a shorter square pulse at about the same rate. Measurements of both decay and buildup of the emission in response to the generating function were used to determine lifetimes. The measurement techniques are discussed fully in Part I. Absolute intensity and lifetime measurements of the $N_2 1P$ (3, 1) and $N_2^+ M$ (2, 0) bands were used to determine the cross-sections of the two systems.

3. NOMENCLATURE AND THEORY

The volume emission rate of a band ($I_{v'v''}$) with a single lifetime can be represented by

$$I_{v'v''} = N_{v'} A_{v'v''} \tag{1}$$

where $N_{v'}$ is the population density of the excited molecules and $A_{v'v''}$ is the spontaneous transition probability of the band. The natural damping constant $A_{v'}$ is related to the natural lifetime by

$$A_{v'} = 1/\tau_{v'} = \sum_{v''} A_{v'v''}. \tag{2}$$

$I_{v'v''}$ may also be written

$$I_{v'v''} = g_{v'}\left(\frac{A_{v'v''}}{A_{v'}}\right), \tag{3}$$

provided the excited molecules do not suffer radiationless deactivation, where $g_{v'}$ is the population rate of the excited levels. For excitation by electrons $g_{v'}$ can be written

$$g_{v'} = \sum_{v'''} N_{v'''} F_e Q_{v'v'''}, \tag{4}$$

where $N_{v'''}$ is the population density of the ground state, F_e is the electron flux, and $Q_{v'v'''}$ the excitation cross-section.

The symbol ϕ is used to describe the damping constant wherever an equation of the form

$$\frac{dN_{v'}}{dt} = -N_{v'}(A_{v'} + D_{v'}) = -N_{v'}\phi_{v'} \tag{5}$$

describes the decay of the population density, where $D_{v'}$ is the probability of radiationless deactivation. A measurement of $I_{v'v''}$ and $\phi_{v'}$ at a single pressure thus allows the calculation of $Q_{v'v''}$ provided $A_{v'}$ is known; $Q_{v'v''}$ can be obtained from $g_{v'}$, through the equation

$$I_{v'v''} = g_{v'}\left(\frac{A_{v'v''}}{\phi_{v'}}\right). \tag{6}$$

A consideration important to the following discussion is that in some cases the generalized Stern–Volmer factor $(A_{v'}/\phi_{v'})$ may be pressure independent and still be measurably less than 1. A direct lifetime measurement is essential in such cases for the determination of excitation cross-sections. This is true of the $N_2^+ M$ system, which we discuss in the following sections.

According to the present work, molecules in the $B\,^3\Pi_g$ state are subject to afterglow effects at low pressures. Equation (5) is thus not applicable for some vibrational levels and one must write

$$\frac{dN_{v'}}{dt} = -N_{v'}(A_{v'} + D_{v'}) + [N_2][N_2A]_{v'}k(v'), \tag{7}$$

where $[N_2]$ is the population density of the ground state molecules, $[N_2A]_{v'}$ is the population density of the precursors, and $k(v')$ is the rate coefficient for the production of $[N_2B](B\,^3\Pi_g)$ molecules. According to the present analysis the population density $[N_2A]_{v'}$ becomes essentially independent of $[N_2]$ at relatively low pressures and the steady state version of equation (7) is then indistinguishable from that of equation (5). Thus, in this pressure region, the presence of an afterglow would not be detectable in observations of steady-state excitation.

4. RESULTS

A. *The $N_2$2PG*

Figure 1 shows the measured excitation function of the (0, 0) band, translated from the present absolute measurements of the (0, 2) band. The measurements of Ref. (5, 6) and the present work are in very good agreement at low electron energies, apart from the 1 eV

difference in position of the Ref. (5) function. The location in energy of the present function (Peak at $E = 14.7$ eV) was determined relative to the known threshold energy of the $N_2^+ 1N(0, 0)$ band. The relative cross-sections of the $N_2 2P(0, 0)$ and (0, 2) bands were obtained from the relative transition probability tables of WALLACE and NICHOLLS[24] (cf. Part I). The probabilities of Ref. (24) are in very good agreement with the measurements of TYTE,[25] Ref. (5), Skubenich and Zapesochnyi (cf. Ref. 5), and thus seem to be well established. However, the Ref. (6) measurements show a marked disagreement with the Ref. (24) probabilities.

Table 1 shows the predicted relative population rates for the ($C\ ^3\Pi_u - X\ ^1\Sigma_g^+$) transition, along with the experimental relative rates and cross-sections. The experimental relative g_v

TABLE 1. CROSS-SECTIONS AND RELATIVE POPULATION RATES DUE TO ELECTRON EXCITATION OF THE $N_2\ C\ ^3\Pi_u$ STATE

$g_{v'}$

v'	1	2a	2b	3	4a	4b	5	6	7	8
	Theoretical	Experimental, laboratory							Aurora	
0	100	102	86	101	91	96	101		94	97
1	55	52	63	53	63	59	49		52	56
2	20	20	27	21	21	20	20		23	21
3	5.8						8		11	
4	1.6						4			
$QC_{v'}(\times 10^{-17}\ \text{cm}^2)$*										
0			2.54	1.40		2.35		2.1		
1			1.86	0.80		1.44		1.15		
2			0.79	0.30		0.49		0.42		
3								0.12		
	$\Sigma QC_{v'}$		5.2	2.5		4.3		3.8		

Cols. 1–8: relative $g_{v'}$ normalized to same total, $\Sigma_{v'} g_{v'}$.
1. $C\ ^3\Pi_u - X\ ^1\Sigma_g^+$ Franck–Condon factors (BENESCH *et al.*[26]).
2a. JOBE *et al.*,[6] $\Delta v = -2$ sequence.
2b. JOBE *et al.*[6] experimental totals of $v'' -$ progressions.
3. SKUBENICH and ZAPESOCHNYI (cf. Ref. 5), $\Delta v = -2$ sequence.
4a. BURNS *et al.*,[5] $\Delta v = -2$ sequence.
4b. BURNS *et al.*[5] experimental totals of $v'' -$ progressions.
5. TYTE[25] experimental totals of $v'' -$ progressions.
6. This work, based on measured (0, 2) band and theoretical relative $g_{v'}$.
7. BROADFOOT and HUNTEN,[27] $\Delta v = -2$ sequence.
8. HUNTEN and SHEPHERD,[28] $\Delta v = -2$ sequence.
* Peak cross-sections.

values agree very well on the whole with the theoretical rates predicted by the Franck–Condon factors[26] for the excitation transition. The relative rates calculated from the $\Delta v = -2$ sequences of Refs. (5) and (6) are shown in Cols. 2a and 4a to illustrate the discrepancy that arises within the measurements of Ref. (6). Cols. 2b and 4b show the relative rates determined from the summation ($\Sigma_{v''} I_{v'v''}$) of the experimental measurements over the whole progression. The good agreement of Col. 2a and the poor agreement of Col. 2b

with the theoretical rates suggests that Ref. (6) may have had a calibration error in relative spectral response. The corresponding Skubenich and Zapesochnyi (cf. Ref. 5) results are almost identical and only a single set of numbers is given in Col. 3. The averaged auroral measurements of BROADFOOT and HUNTEN[27] and HUNTEN and SHEPHERD[28] shown in Cols. 7 and 8, although potentially less accurate, also agree remarkably well with the theoretical rates for the first three levels.

The total peak cross-section estimates ($QC = \Sigma_{v'} QC_{v'}$) are not in complete agreement (Table 1). The present estimate ($QC = 3.8 \times 10^{-17}$ cm^2) which is based on the measured $QC_{0,2}$ value and the apparently well established theoretical relative rates $g_{v'}$, is in good agreement with Ref. (5). The Skubenich and Zapesochnyi estimate is about a factor of 1.5 lower. The Ref. (6) estimate is uncertain due to the factors discussed above. The validity of the present estimate of QC will be discussed further in the next subsection in reference to the excitation of the $B\,^3\Pi_g$ state.

The present measurements of the excitation function above 25 or 30 eV, along with those of Refs. (5–8), appear to be untrustworthy. There is general disagreement among the various measurements at higher electron energies. The most plausible explanation of the discrepancy may be the presence of low energy electrons reflected from the collector of the electron gun, especially in those cases where a columnating magnetic field was employed. The measurements by AARTS *et al.*[29] above 50 eV, shown in Fig. 1, give the lowest cross-sections of all and may be the least affected by secondary electrons. There is no reason to doubt the calibration of the (Ref. 29) work since their measured cross-section of the $N_2^+ 1N(0, 0)$ band is in comparatively good agreement with the accepted values.

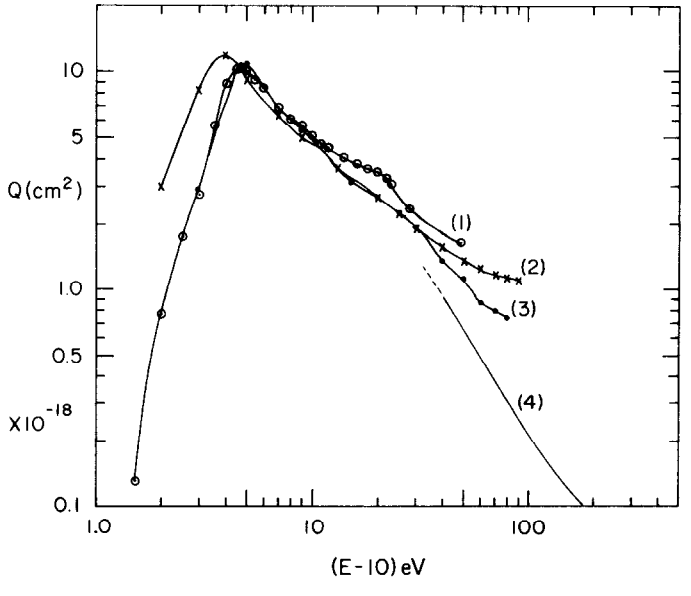

FIG. 1. Excitation function of the $N_2 2PG(0, 0)$ band.* 1. This work. 2. BURNS *et al.*[5] 3. JOBE *et al.*[6] 4. AARTS *et al.*[29]

* The abscissa is the electron energy (E) minus 10 eV.

B. The $N_2 1PG$

The measured excitation function of the $N_2 1PG(3, 1)$ band in the low energy region is given in Fig. 2. The function includes a fraction of the ($C\,^3\Pi_u - X\,^1\Sigma_g^+$) excitation transition through radiative decay in the $N_2 2PG$ as well as direct excitation to the $B\,^3\Pi_g$ state. The

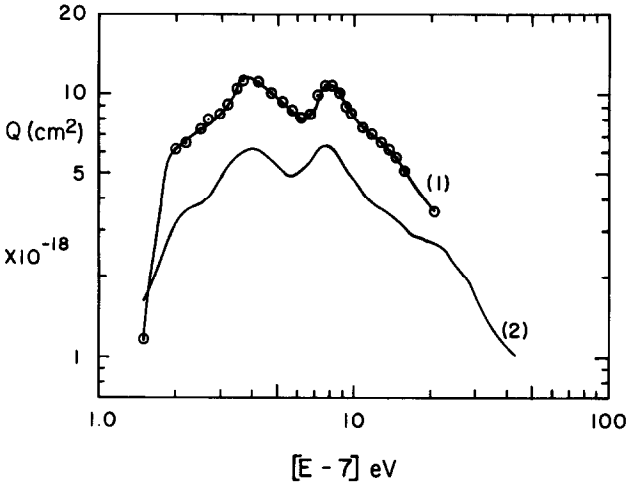

FIG. 2. Excitation function of the $N_2 1PG(3, 1)$ band. 1. Present work. 2. STANTON and ST. JOHN.[2]

peak of the $B\,^3\Pi_g v = 3$ level is estimated to be at 10.8 eV. The other peak at 14.8 eV is due to the $C\,^3\Pi_u$ state. The measurement by STANTON and ST. JOHN[2] also shown in the figure contains about the same relative cascade contribution but is roughly a factor of 2 lower in magnitude than the present estimate. The measurement by MCCONKEY and SIMPSON[1] is not shown but is similar in magnitude to that of Ref. (2). For reasons discussed earlier the present cross-section measurements were determined with the aid of lifetime measurements. Measurements of ϕ at three pressures for the $B\,^3\Pi_g v = 3$ level are shown in Fig. 3. The energy of the exciting electrons was below the threshold of the $C\,^3\Pi_u$ state. In sharp contrast to the lifetime measurements by JEUNEHOMME,[9] and WENTINK *et al.*,[30] the decay curves for $P = 0.5\,\mu$, $9\,\mu$ show only a single damping constant. The pulsed electrodeless discharge measurements by Refs. (9, 30) in the same pressure region as the present work indicated substantial secondary contributions. However, the present measurement at $P = 50\,\mu$ contains a longer lived component ($\phi = 5.0 \times 10^4\,\text{sec}^{-1}$) which contributes about 36 per cent of the total intensity of the $B\,^3\Pi_g v = 3$ level. The secondary decay which has about the same damping constant as one of the components measured by Jeunehomme, appears rather abruptly in the region $P = 10-50\,\mu$ and must be at least second order in $[N_2]$; there is no indication of more than one damping constant over 2 decades of the decay at $P = 9\,\mu$. The measurements of Refs. (9, 30) indicated two secondary components, but it is possible this may be due to a single non-exponential afterglow. Unfortunately the present measurement at $P = 50\,\mu$ was not accompanied by relative band intensity measurements. The measurements shown in Fig. 3 were made by gating the electron beam off and by observing the radiative decay with a sampling gate, as described in Part I. The curvature

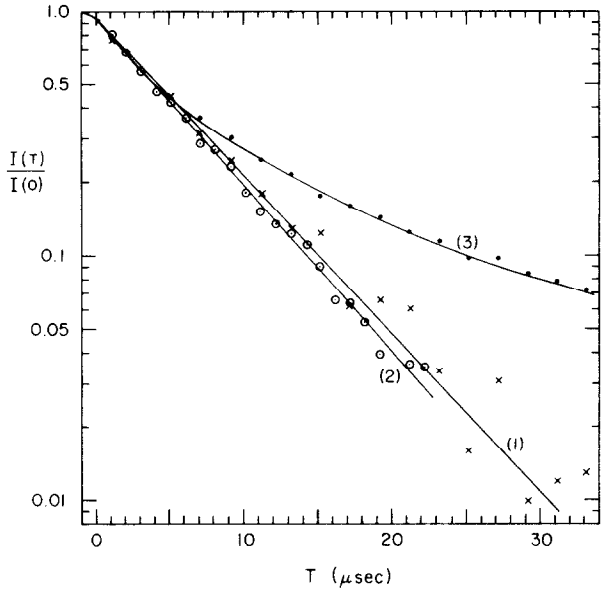

FIG. 3. Lifetime $N_2 1PG(3, 1)$ band. 1. $\phi = 0.151 \times 10^6$ sec^{-1}, $P = 0.5\ \mu$. 2. $\phi = 0.161 \times 10^6$ sec^{-1}, $P = 9\ \mu$. 3. $\left.\begin{matrix}\phi_1 = 0.272 \times 10^6 \text{ sec}^{-1}, \alpha_1 = 0.641 \\ \phi_2 = 0.050 \times 10^6 \text{ sec}^{-1}, \alpha_2 = 0.359\end{matrix}\right\} P = 50\ \mu$.

near $t = 0$ is due to the finite width of the sampling gate. Observations of the build-up of the emission rate by gating the electron beam on, indicated no measurable difference in lifetime at a given pressure. We therefore conclude that the $B\,^3\Pi_g v = 3$ population at $P < 10\ \mu$ was controlled entirely by the primary excitation process, radiative decay, and a small amount of collisional deactivation by N_2. The extrapolated lifetime of the $v = 3$ level is not significantly different from the measurement at $P = 0.5\ \mu$, and it was not necessary to determine the excitation function shown in Fig. 2, by extrapolation. The deactivation rate coefficient for N_2, obtained from these measurements is 7.6×10^{-11} cm^3/sec. The estimated natural lifetime of the $B\,^3\Pi_g v = 3$ level (6.5×10^{-6} sec) determines the lifetimes of the remaining levels through the relative transition probability measurements discussed in Part I. The results are in very good agreement with the values obtained by Jeunehomme and others (cf. Part I).

The population rates of the $v < 5$ levels show no consistent variation relative to the $v = 3$ level in the pressure region $P = 0.5\ \mu$–$10\ \mu$ (cf. Table 2). In fact the relative population rates of the lower levels agree rather well with the rates predicted by the Franck–Condon factors for the ($B\,^3\Pi_g - X\,^1\Sigma_g^+$) transition. However the $v > 4$ levels display a variation in population rate as a function of pressure relative to the $v = 3$ level. The pressure dependence is detectable by visual inspection of the spectra. Figure 4 shows superposed observations of the $\Delta v = 3, 4, 5$ sequences at $P = 0.5\ \mu$, $2\ \mu$, and $10\ \mu$. The relative intensities of the $v = 3$ and 4 levels do not change but the higher levels show a greater development than predicted by the ($B\,^3\Pi_g - X\,^1\Sigma_g^+$) Franck–Condon factors, and vary with pressure in a manner consistent with the presence of an afterglow; since we have established that g_3 for the $B\,^3\Pi_g$ state is first order in $[N_2]$, the pressure variation of $g_{v>4}/g_3$ indicates a higher

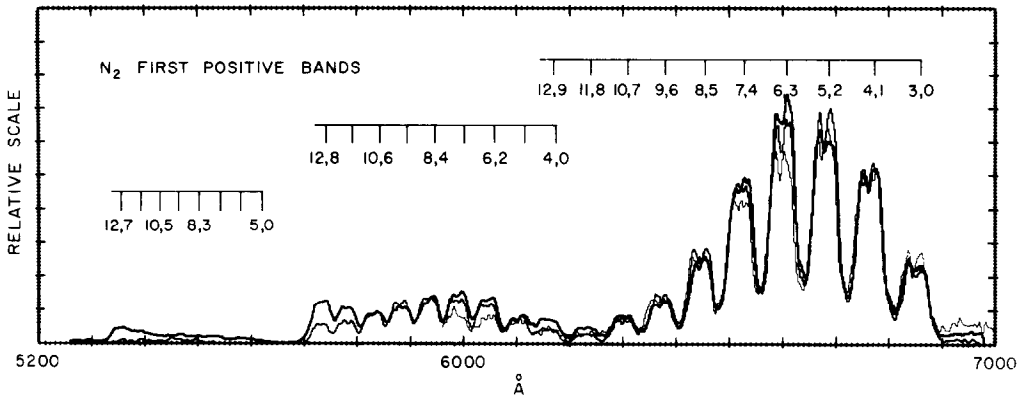

FIG. 4. Spectra of the $\Delta v = 3, 4, 5$ sequences of the $N_2 1PG$. 1. Heavy trace $P = 10\,\mu$. 2. Medium trace $P = 2\,\mu$. 3. Light trace $P = 0.5\,\mu$.

order dependence for the $B\,^3\Pi_g v > 4$ levels. The variation is most noticeable in the $v = 6$, 11, 12 levels. Note that the vibrational development ends abruptly at $v = 12$, the first level below the dissociation limit for N_2. Table 2 shows the measured relative population rates of the $B\,^3\Pi_g$ levels at various pressures and incident electron energies. Included in the table are relative rates of earlier publications recalculated using the transition probabilities given by Part I. The rates are given for the peaks of the excitation functions in order to reflect the relative apparent cross-sections of the levels. This required an adjustment of the present measured intensities for the $E = 11.5$ eV case due to the differences in position of the excitation functions. The theoretical relative rates determined by the Franck–Condon factors for the excitation transitions (Ref. 26) are given in Cols. 11, 12. Column 11 includes an arbitrary contribution from the $C\,^3\Pi_u$ state determined by a total cross-section ratio of $QC/QB = 0.20$. Column 12 is due entirely to the $(B\,^3\Pi_g - X\,^1\Sigma_g^+)$ transition. Most of the effect of cascade appears in the relative rates of the lower vibrational levels. The measured relative rates (g_v), with the exception of Col. 10, all clearly indicate a greater vibrational development than the predicted values in Cols. 11, 12. The measurements of the present work (Col. 1–7) show a general tendency for the apparent g_v values to approach the predicted values with decreasing pressure. This is shown most clearly by the plotted values of the $B\,^3\Pi_g v = 6$, 11 levels relative to the $v = 4$ level, IB_6/IB_4 and IB_{11}/IB_4, shown in Fig. 5. The ratios predicted by the theoretical relative cross-sections QB_v/QB_4 are indicated in the Figure. The important characteristics of the afterglow are illustrated in this Figure: (1) Most of the variation of IB_v/IB_4 takes place at pressures below about $P = 3\mu$. The afterglow is almost first order in $[N_2]$ above $P = 3\,\mu$ and shows a quadratic tendency only at the lower pressures. (2) There is very little dependence on electron energy. The precursor to the afterglow contribution must therefore have a very similar excitation function to that of the $B\,^3\Pi_g$ state. The direct electron excitation rates of the levels vary considerably between $E = 11.5$ eV–100 eV, due to the peculiar shape of the excitation function, typical of electron exchange transitions. The effect of cascade from the $C\,^3\Pi_u$ state can be neglected in these levels. The smooth curves drawn through the plotted points in Fig. 5 are theoretical calculations to be discussed in the following section.

TABLE 2. RELATIVE POPULATION RATES AND ELECTRON CROSS-SECTIONS OF THE N_2 1PG

Col.	1	2	3	4	5	6	7	8	9	10	11	12	13	14	15
E(ev)	11.5			17.0		100					Theoretical		$QB_{v'}$(cm^2)		
$P(\mu)$	0.5	2	10	2	10	0.5 → 1	3 → 28								
$v'=0$								51			123	58	7.3–18	3.9–18	
1	149	132	129	161	155	180	162	103			161	139	1.8–17	8.0–18	
2	165	186	182	182	181	185	190	164	149		188	183	2.3–17	1.3–17	1.4–17
3	173	164	157	155	147	169	160	162	173	217	174	179	2.3–17	1.4–17	1.7–17
4	127	132	131	124	123	121	120	142	140	134	135	142	1.8–17	1.2–17	1.4–17
5	92	94	98	92	94	87	93	117	99	88	93	99	1.3–17	8.5–18	1.0–17
6	60	69	74	69	78	56	70	85	69	58	57	62	7.8–18	6.4–18	6.9–18
7	51	49	50	46	52	36	41	53	43	35	34	37	4.6–18	3.8–18	4.2–18
8	29	29	31	27	26	29	28	30	23	22	19	20	2.6–18	2.2–18	2.2–18
9	18	18	21	17	17			17	12		9.7	11	1.4–18	1.4–18	1.0–18
10	11	13	15	11	13			11	5.9		4.9	5.5	7.0–19	8.4–19	6.1–19
11	3.7	9.5	12	8.1	12			7.7	3.6		2.4	2.7	3.6–19	5.9–19	3.8–19
12	0.9	11	12	9.3	15			7.0			1.2	1.4	1.8–19	4.7–19	
κ_{12}	*4.0–3	3.6–3	5.8–3	7.3–3	1.0–2	1.0–2	6.7–3	1.3–2	4.7–3	5.1–4	1.7–2	0	$\Sigma QB_{v'}$		
κ_{11}	4.1–3	6.5–3	9.5–3	3.9–3	8.3–3	3.0–3	2.9–3	4.0–2	8.8–3	5.7–4	0		1.2–16		

* 4.0×10^{-3}.

Cols. 1–12: Normalized to same total rate ($\Sigma_{v'} g_{v'}$). Cols. 1–7. Present work. The relative rates of Cols. 1–5 are adjusted to reflect the relative peak values of the excitation functions.

8. Peak relative rates due to STANTON and ST. JOHN.[2]
9. Peak relative rates due to MCCONKEY and SIMPSON.[1]
10. Relative rates from weak high altitude aurora due to SHEMANSKY and VALLANCE JONES.[19]
11. Theoretical relative rates of ($B\,^3\Pi_g - X\,^1\Sigma_g^+ v = 0$) with ($QC/QB = 0.20$) contribution from ($C\,^3\Pi_u - X\,^1\Sigma_g^+ v = 0$).
12. Theoretical relative rates of ($B\,^3\Pi_g - X\,^1\Sigma_g^+ v = 0$).
13. Peak cross-sections ($B\,^3\Pi_g - X\,^1\Sigma_g^+ v = 0$), present work (see text).
14. Peak cross-sections ($B\,^3\Pi_g - X\,^1\Sigma_g^+ v = 0$) STANTON and ST. JOHN[2] (see text).
15. Peak cross-sections ($B\,^3\Pi_g - X\,^1\Sigma_g^+ v = 0$) MCCONKEY and SIMPSON[1] (see text).

Cross-correlation factor κ, (Eq. 8), of Cols. 1–10 with Cols. 11, 12. Levels $v = 4$–8 only were used in the computation of κ for Col. 10.

The last two rows of Table 2 are numbers (κ) representing a quantitative cross-correlation of the theoretical rates given in Cols. 11, 12, with the measured rates given in Cols. 1–10. The cross-correlation factor (κ) is given by the following equation:

$$\kappa = \left[1 - \frac{\Sigma g_x g_y}{(\Sigma g_x^2 \Sigma g_y^2)^{1/2}}\right]. \tag{8}$$

Thus the smaller values of κ represent a greater correspondence between the two sets of numbers. A value of κ for the correlation of the two theoretical sets is given (1.7×10^{-2}) in order to indicate the significance of the relative magnitudes of the numbers. A value $\kappa = 1 \times 10^{-3}$ or lower with this particular group of numbers would represent a residue due only to measurement statistics, and a very good correlation. The general trend in the values of κ toward better correlation as a function of decreasing pressure is another indicator

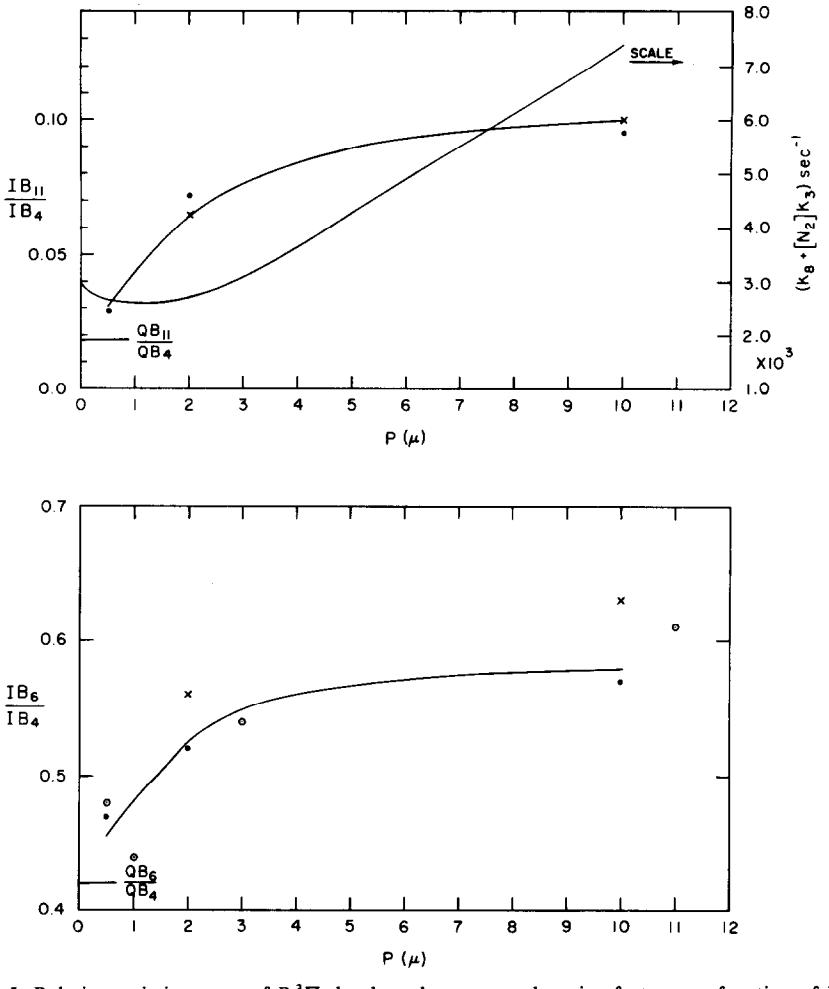

FIG. 5. Relative emission rates of $B\,^3\Pi_g$ levels and precursor damping factor as a function of N_2 pressure. ● Measured points at electron energy $E = 11.5$ eV. × Measured points at $E = 17$ eV. ⊙ Measured points at $E = 100$ eV. Solid curves are theoretical calculations.

of the results shown in Fig. 5. The effect of cascade from the $C\,^3\Pi_u$ state is also evident; the relative rates at $E = 11.5$ eV, which contain no cascade contribution, display a better correlation with the values of Col. 12, whereas the rates at $E = 17$ eV and $E = 100$ eV correlate better with the values of Col. 11. Correlation of the $v = 1$–4 levels at $E = 11.5$ eV, which contain no measurable afterglow contribution, give values of $\kappa_{12} = 10^{-3}$–10^{-4} indicating excellent agreement with the theoretical rates for the $(B\,^3\Pi_g - X\,^1\Sigma_g^+)$ transition. The measurements of high altitude weak aurora[19] are also in excellent agreement with the rates of Cols. 11, 12 for the $v = 4$–8 levels. The values κ_{11} and κ_{12} are almost equal in this case since cascade from the $C\,^3\Pi_u$ state has a negligible effect on the relative rates of the $v > 3$ levels. The $v = 3$ level has been ignored (Col. 10) because of anomalous behavior in the aurora (cf. Ref. 19). Thus the trend in the laboratory measurements at the lowest pressures and the high altitude auroral measurements lead to the conclusion that the relative

excitation rates of the ($B\,^3\Pi_g - X\,^1\Sigma_g$) transition due to electron impact are well represented by the theoretical rates. The earlier laboratory measurements by STANTON and ST. JOHN[2] and MCCONKEY and SIMPSON[1] have been reduced using the transition probabilities of Part I, and the relative rates are given in Cols. 8 and 9. These numbers represent measurements at the peaks of the excitation functions and contain no contribution due to cascade from the $C\,^3\Pi_u$ state. This is reflected in the fact that $\kappa_{12} < \kappa_{11}$ for both sets of values. The relative values of both sets fall somewhere between the extremes of the present work. Indeed, the spectra shown by Ref. (2) have a very similar appearance to those of the present work; the Ref. (2) band intensity measurements in each v''-progression, are in excellent agreement with the transition probabilities of Part I. However, this is not true of the Ref. (1) measurements. The relative population rates depend somewhat on the particular bands chosen for the reduction, and for this reason the values of Col. 9 are uncertain. The particular bands chosen here were those of the $\Delta v = 3$ sequence and the (2, 0) band. It is not clear whether or not there was a difference in calibration of spectral sensitivity with the present work. It should be noted that the measurements of Ref. (1) appear to have been made by using a spectrometer essentially as a filter photometer rather than in the scanning mode. We do not regard this as conducive to accurate measurement in view of the degree of blending of the bands. The relative values of Cols. 8 and 9 suggest that the earlier experiments also were affected by the afterglow described here. According to the interpretation given in the following section, the afterglow would be very difficult to avoid in any experimental arrangement.

The peak values of the excitation cross-sections ($QB_{v'}$) due to the present work, Ref. (2) and Ref. (1), are given in Cols. 13, 14, and 15 respectively. As we have indicated above, the present relative cross-sections correspond to the relative theoretical rates (Col. 12). The $QB_{v'}$ values calculated in the present work, from the individual band cross-sections given by Ref. (2) (Table 2 Col. 14) differ from their own values due to the erroneous transition probabilities assumed in their calculations. Since it seems fairly certain that the Ref. (1) and (2) cross-sections contain afterglow contributions, the comparison of cross-sections is restricted to the lower vibrational levels. The Ref. (1) values are slightly larger than those of Ref. (2), but both are roughly a factor of 1.5 lower than the present estimates. The excellent agreement of the Ref. (2) measurements with the relative transition probabilities of Part I indicates that the relative spectral sensitivity calibrations were the same in the two cases. Thus it is improbable that the absolute sensitivity calibrations would differ. A more plausible reason for the discrepancy arises in the relatively long lifetimes of the $B\,^3\Pi_g$ state. The excited molecules move an average of 0.3 cm–0.4 cm during their lifetimes. As a result the volume emission rates would be measurably different from the volume production rates because of the relatively small diameter electron beams used in the laboratory experiments. Measurements made with slits aligned along the beam could be affected by the difference between volume emission and production rates, depending on the size of the image at the beam. There is no discussion of $B\,^3\Pi_g$ state lifetimes in any of the earlier publications.

The total peak excitation cross-section estimated in the present work is 1.2×10^{-16} cm^2 as given in Table 2. The totals due to Refs. (1) and (2) are not given because the higher levels appear not to be due entirely to primary excitation. In the present work, for example, the afterglow process is responsible for about 90 per cent of the emission in the $B\,^3\Pi_g v = 12$ level at pressures $P > 3\ \mu$.

The fact that the $B\,^3\Pi_g$ state is the lower state of the $N_2 2PG$, allows a measure of the cross-section ratio QC/QB independent of the absolute spectral sensitivity calibration of the spectrometer. The relative population rates of the lower levels of the $B\,^3\Pi_g$ state are measurably affected by the ($C\,^3\Pi_u - B\,^3\Pi_g$) transition (cf. Part I, Table 2). Since the relative population rates of the $C\,^3\Pi_u$ state and the transition probabilities of the $N_2 2PG$ appear to be well established, the relative population rates of the $B\,^3\Pi_g$ levels can be calculated with a good degree of accuracy. One can then compare these calculated rates for various ratios (QC/QB), with the observations. In the computation described below, the average of the experimental measurements given in Cols. 2 and 3 of Table 2 were used to represent the direct excitation rates of the $B\,^3\Pi_g$ state, in order to cancel out the effects of the afterglow contribution. The calculated rates due to cascade were then added to the direct rates and the result was compared with the spectra obtained at the higher electron energies (Cols. 4–7, Table 2). Figure 6 shows the plotted values of the cross-correlation factor κ (equation 8) as a function of QC/QB. The numbered curves correspond to the columns of Table 2. Columns 6 and 7 represent averages of spectra obtained within the indicated pressure ranges. The individual spectra were used in the calculation of the Fig. 6 curves, and are indicated by the lower case letters. All but two of the curves show minima in the region $QC/QB = 0.25$–0.29. The spectra that tend to give the larger values of QC/QB (6a, 6b) are low pressure spectra containing smaller afterglow contributions and with higher noise levels than the spectra of Cols. 2 and 3. The broad minima and the shift to higher values of QC/QB are consistent with these two effects. We therefore ignore the 6a and 6b curves in making an estimate of QC/QB. The average value is estimated to be $QC/QB = 0.27$. The cross-section ratio at the peaks of the excitation functions as determined from the direct measurements of the present work (Tables 1, 2) is $(QC/QB)_{\text{Peak}} = 0.32$. The larger value at the peaks of the excitation functions is consistent with a tendency observed in the direct measurement of the excitation functions of the two systems; the $C\,^3\Pi_u$ excitation function appears to decrease at a slightly higher rate than that of the $B\,^3\Pi_g$ state as a function of energy above the peak value. The two results are thus considered to be in very good agreement. The curve labled (2 + 3) is included in Fig. 6 in order to illustrate the variation of κ as a function of (QC/QB) for the case of perfect correlation (at $QC/QB = 0$). The magnitudes of κ at the minima for the curves used in the estimation of QC/QB are all in the 10^{-3}–10^{-4} region suggesting that the errors could easily be due entirely to measurement noise.

It has been pointed out above that the $B\,^3\Pi_g$ excitation functions as measured by Refs. (1, 2) appear to contain about the same relative contributions from the $C\,^3\Pi_u$ state (cf. Fig. 2), as the present measurements. But we are in disagreement in the estimate of the magnitude of the $B\,^3\Pi_g$ excitation function, whereas the present measurement of the $N_2 2P(0, 0)$ is in good agreement with those of the same two groups (Refs. 5, 6). Thus according to the present calculations, the measurements of Refs. (1, 5) and Refs. (2, 6) are not consistent in respect to the QC/QB ratio.

ZAPESOCHNYI and SKUBENICH[7] and SKUBENICH and ZAPESOCHNYI[8] present measurements of the total $B\,^3\Pi_g$ excitation function. Ref. (7) gives a peak value of 1.4×10^{-16} cm^2 and Ref. (8)—1.0×10^{-16} cm^2. No explanation for the difference between the two measurements is given in the later work (Ref. 8). Few details are available for these measurements, and a comparison with the present work may not be valid; the transition probabilities used for the estimates were not based on a measured electronic transition moment and do

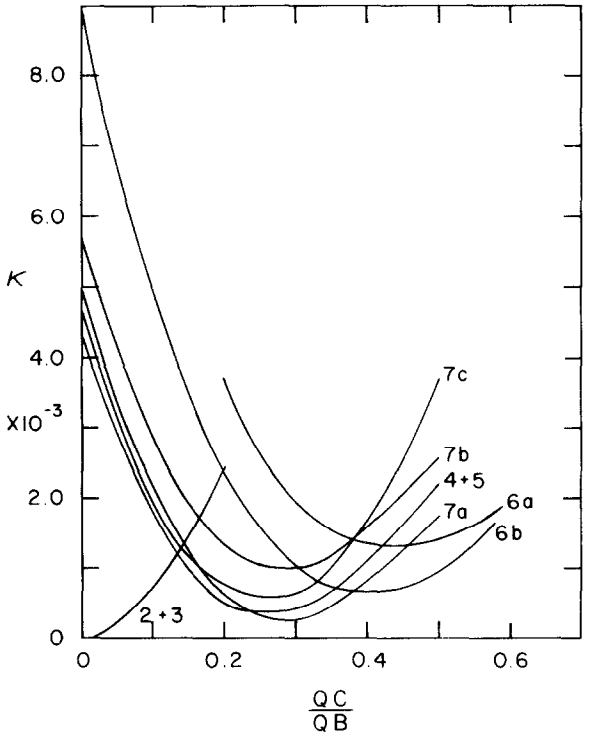

FIG. 6. Cross-correlation factor κ vs. QC/QB.* $\kappa = \left[1 - \frac{\Sigma g_x g_y}{(\Sigma g_x^2 \Sigma g_y^2)^{1/2}}\right]$, equation (8), $x = (2+3)+$ cascade contribution from $C\,^3\Pi_u$, y = rates due to spectra in the indicated columns of Table 2. (2+3) average of rates in Cols. (2, 3). (4+5) average of rates in Cols. (4, 5). 6a $P = 0.5\,\mu$, 6b $P = 1\,\mu$, 7a $P = 3\,\mu$, 7b $P = 11\,\mu$, 7c $P = 28\,\mu$.

* See text.

not correspond to those given by Part I. No measurements of individual bands were given in either work.

C. *The N_2^+M system*

The intensity of the N_2^+M system relative to the N_2^+1N system at a given electron energy as observed in the present work, increases approximately linearly with decreasing pressure down to a point somewhere between $P = 1\,\mu$ and $2\,\mu$, where a sudden change takes place. This appears to be a characteristic common to all of the published laboratory observations in which information is presented in sufficient detail. The N_2^+1N system is known to be well behaved at least at pressures below $P = 30\,\mu$, because of the short lifetime of the $B\,^2\Sigma_u^+$ state, and the intensity is proportional to $[N_2]$ and the electron current. The N_2^+M system is therefore subject to radiationless deactivation at least down to pressures in the $P = 1$–$2\,\mu$ region. All of the previous work in which cross-section estimates are given[4,2,3,7,8] is based on the assumption that the approximate first order dependence on $[N_2]$ and on F_e in the lower pressure regions implies the absence of radiationless deactivation. However this is not true of the present experiment. As we shall discuss below,

similarities between the present observations and the earlier work suggest that radiationless deactivation was also significant in the latter case at low pressures, and has led to erroneous cross-section measurements.

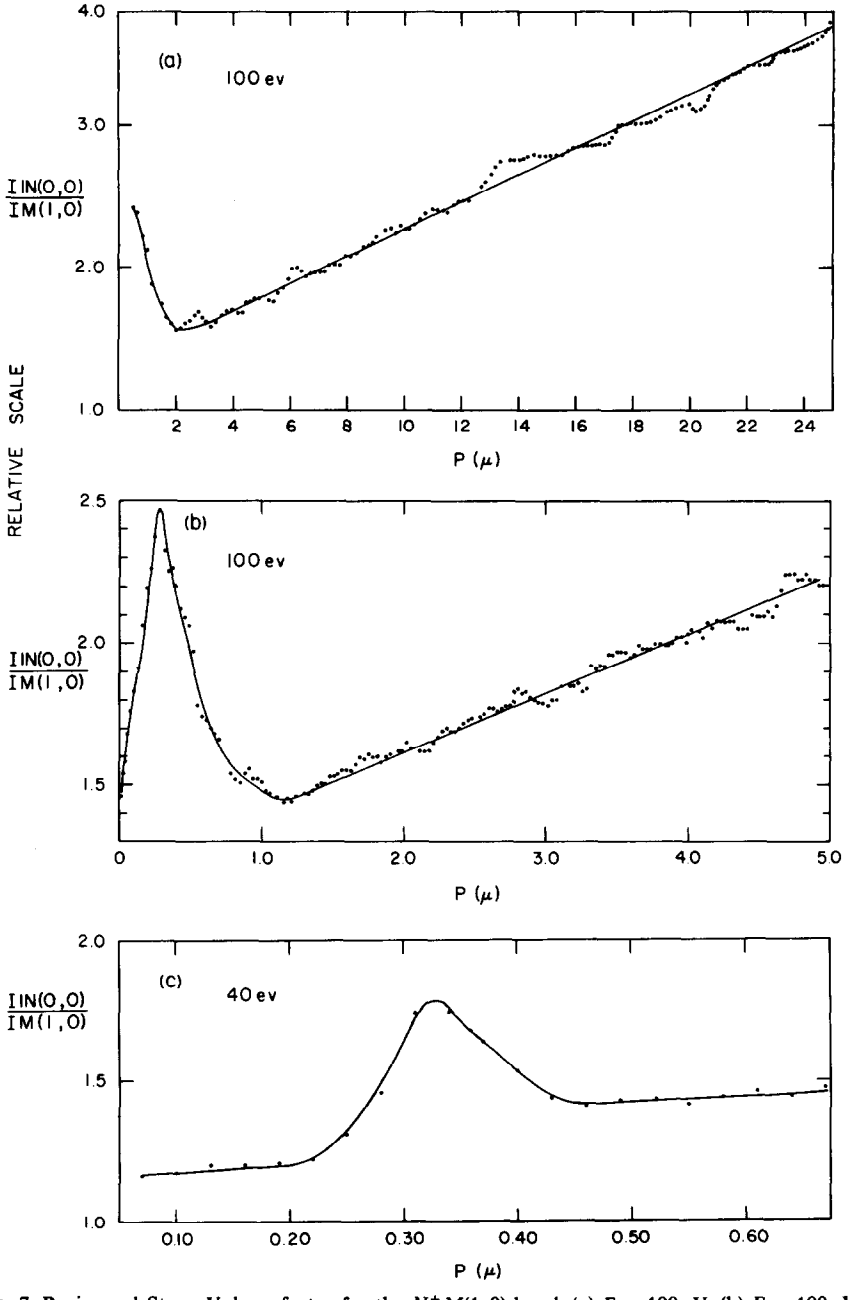

FIG. 7. Reciprocal Stern–Volmer factor for the $N_2^+ M(1,0)$ band. (a) $E = 100$ eV. (b) $E = 100$ eV. (c) $E = 40$ eV. Curves were obtained at a constant production rate for the $N_2^+ 1N(0,0)$ band.

Figure 7 shows the reciprocal Stern–Volmer factor (ϕ) for the $N_2^+ M(1, 0)$ band as represented by the ratio $I1N(0, 0)/IM(1, 0)$. The curves were produced at a constant production rate for the $N_2^+ 1N(0, 0)$ band, and therefore $F_e(\alpha 1/P)$ increased rapidly at the lower pressures. The observations were made during a continuous pressure scan. The small scale fluctuations are due to fluctuations in the pressure scan control system. The large resonance in the deactivation rate of the $A\ ^2\Pi_u$ level at about $P = 0.3\ \mu$ appears to be due to the presence of the columnating magnetic field. The magnitude and width of the feature depends on the primary electron energy as the difference between curves (a) or (b) and (c) illustrates. Note that in the pressure region surrounding the resonance in curve (c), ϕ is almost independent of pressure. The sudden departure at $P \approx 1\ \mu$ from an almost linear dependence of ϕ on P is true of the earlier work in which measurements of this kind are described.[4,14] According to the Ref. (4) observations ϕ became approximately independent of P at pressures $P < 1.5\ \mu$. The Ref. (14) measurements indicated a sudden increase in the apparent radiationless deactivation coefficient in the same pressure region. In this case the data was obtained through intensity and phase measurements with a modulated electron beam. STANTON and ST. JOHN[2] and SRIVASTAVA and MIRZA[3] do not discuss the Stern–Volmer factor, but appear to have obtained results similar to those of Ref. (4) and the present work in the pressure region $P < 2\ \mu$, in which ϕ was approximately independent of pressure. This apparently was what led the authors of Refs. (2–4) to the assumption that $\phi_v = A_v$ in the appropriate pressure region. However the Stern–Volmer plots of Fig. 7, Ref. (2), and Ref. (14) cannot be interpreted physically in terms of an abrupt disappearance of radiationless deactivation. The change in slope in the $P = 1$–$2\ \mu$ region can be reasonably explained only as a change in the pressure dependence of a finite effective deactivation coefficient. This is confirmed by the lifetime measurements discussed below. The damping factor ϕ observed in the present experiment also displays an electron current dependence, and the plot in Fig. 7 thus contains an additional hidden, variable parameter.

Measurements of the decay of the $N_2^+ M(2, 0)$ band in response to a step function in the electron beam current are shown in Fig. 8. The electron energy was $E = 100$ eV. The damping factor is well defined and decreases uniformly as a function of pressure down to a peak lifetime at about $P = 2\ \mu$, as curves (1), (2), and (3) illustrate. However at lower pressures the emission decays at a higher rate, and becomes non-exponential. The curve (4) at $P = 1\ \mu$ is representative of the decay curves in the low pressure region. The shape of the curve is not characteristic of the presence of an afterglow since the effective lifetime becomes shorter with increasing decay time. The shortening effect on the lifetime at $P = 1\ \mu$ is somewhat exaggerated relative to the other curves in Fig. 8 due to the use of a higher excitation current. The response to a short excitation pulse at low pressures indicates different effective lifetimes for the build-up and decay portions of the emission, whereas no measurable discrepancy was observed at pressures $P > 2\ \mu$. The current and pressure dependence of the (2, 0) band is shown in Fig. 9. Curve (1) is drawn through the present observations made using an electron current of about 500 μA, curve (2) represents the results at 8 μA, and curve (3) is a straight line drawn through the measurements due to Ref. (14). The measurements do not extend below $P = 2\ \mu$ since the lifetime cannot be defined at lower pressures. Extrapolation to zero pressure in order to obtain an estimate of the natural lifetime of the $A\ ^2\Pi_u$ state is clearly a doubtful procedure in this case. The extrapolated value from curve (2) is $\tau_2 = 4.4\ \mu$sec, and curve (3) gives $\tau_2 = 6.6\ \mu$sec. We do not give an estimate of the deactivation coefficient due to the ill defined nature of the results.

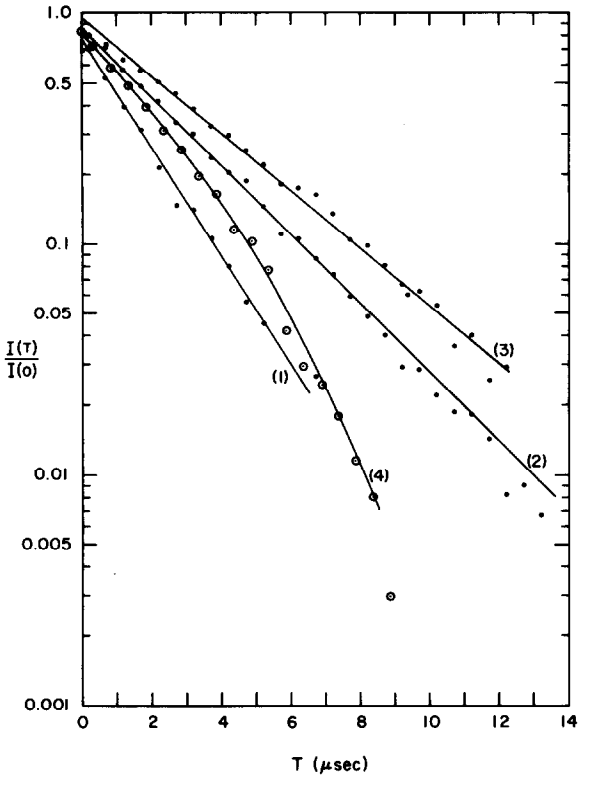

FIG. 8. Lifetime $N_2^+ M(2,0)$ band. $E = 100$ eV. (1) $\phi = 0.54 \times 10^6$ sec^{-1}, $P = 19\ \mu$. (2) $\phi = 0.343 \times 10^6$ sec^{-1}, $P = 6\ \mu$. (3) $\phi = 0.268 \times 10^6$ sec^{-1}, $P = 2\ \mu$. (4) ϕ–variable, $P = 1\ \mu$.

The lifetime measurements also display a dependence on electron energy; the deactivation probability in the present measurements has a tendency to decrease with decreasing electron energy below $E = 100$ eV. Ref. (4) presents steady state Stern–Volmer plots which indicate an increase in ϕ at 80 eV over the value at 120 eV. The uncorrected excitation function thus changes in shape as a function of electron energy and pressure. The various shapes given in earlier publications (cf. Ref. 4) have been approximated in the present measurements with combinations of the parameters. Higher electron currents tend to flatten the shape. At fairly low currents in the region of 20 μA, measurements near the threshold indicated a linear dependence of the cross-section on E. Lower currents tended to increase the energy region over which Q was linear in E. At currents in the region of 1 μA the linear part of the curve appeared to be limited at approximately E = 30 eV. This will be discussed further below.

Table 3 gives the measured relative population rates of the observed $A\ ^2\Pi_u$ levels, in comparison with the theoretical rates determined by the Franck–Condon factors for the ($A\ ^2\Pi_u - X\ ^1\Sigma_g^+ v = 0$) transition (NICHOLLS[31]). Cols. 1–5 are due to the present work at $E = 100$ eV and at the indicated pressures. Note the increase in vibrational development with decreasing pressure. This suggests that the deactivation rate coefficients increase with the vibrational quantum number. The lifetime measurements of Ref. (14) indicate the same

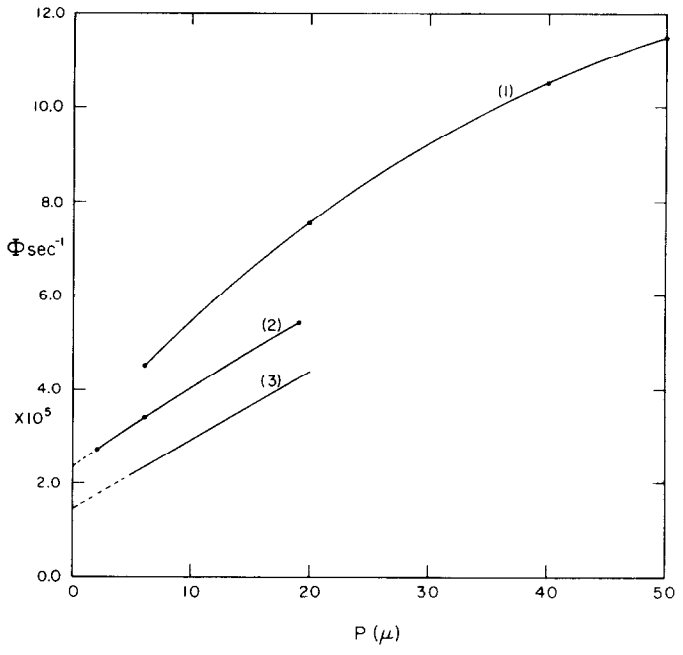

FIG. 9. Damping factor of $N_2^+ M(2, 0)$ band. (1) Present work, Electron current $\approx$ 500 μA, E = 100 eV. (2) Present work; electron current $\approx$ 8 μA, E = 100 eV. (3) O'NEIL and DAVIDSON.[14]

TABLE 3. RELATIVE POPULATION RATES AND EXCITATION CROSS-SECTIONS OF THE $N_2^+ M$ SYSTEM

Column	1	2	3	4	5	6	7	8	9	10
$P(\mu)$	28	11	3	1	0.5				Theory	$QM_{v'}$(cm^2)
$v' = 0$							60		66	3.0–17
1	105	98	97	95	90		85		84	3.8–17
2	59	58	60	58	59	53	66	77	61	2.8–17
3	21	29	27	27	31	39	30	23	33	1.5–17
4	12	12	12	14	15	20	16	10	15	7.0–18
5	3.5	3.4	3.2	5.7	5.9	3.0	7.8		6.5	2.9–18
κ	*1.6–2	6.6–3	6.3–3	5.4–3	1.5–3	1.3–2	2.2–3	2.7–2	0	$\Sigma QM_{v'}$ 1.2–16

* 1.6×10^{-2}.

Cols. 1–8. Experimental, calculated using transition probabilities given by Part I. Cols. 1–5. This work, E = 100 eV. $P_1 = 28\ \mu$, $P_2 = 11\ \mu$, $P_3 = 3\ \mu$, $P_4 = 1\ \mu$, $P_5 = 0.5\ \mu$.

6. SIMPSON and MCCONKEY.[4]

7. STANTON and ST. JOHN,[2] from bands selected for their intensity and relative freedom of blends with other emissions.

8. SRIVASTAVA and MIRZA.[3]

9. NICHOLLS,[31] theoretical rates.

10. Cross-section (cm^2) estimates at 100 eV ($A\ ^2\Pi_u - X\ ^1\Sigma_g^+$) based on present measurements and O'NEIL and DAVIDSON[14] lifetimes.

κ, (Eq. 8), is the correlation factor with the theoretical rates of Col. 9.

trend. Homogeneous deactivation appears to be significant at pressures $P < 3\,\mu$ in the region where the mean free path for thermal molecules would be longer than the radius of the container. This, along with the Stern–Volmer plots and lifetime measurements would be consistent with diffusion by drift in crossed electric and magnetic fields. The last row of Table 3 shows the cross-correlation factor (κ) calculated with the theoretical relative rates of Col. 9. The correlation continues to improve down to $P = 0.5\,\mu$, where the value of κ is in the region of the residual measurement noise. Thus according to the present observations the relative excitation rates are well represented by the Franck–Condon factors for the excitation transition. The relative rates due to SIMPSON and MCCONKEY (Col. 6), recalculated using the transition probabilities of Part I, indicate a poor correlation with Col. 9. The rates due to Stanton and St. John (Col. 7) have a value of κ essentially the same as the present low pressure measurements. However it should be noted that the Ref. (2) measurements of some of the bands did not conform well to the transition probabilities, and the rates given in Col. 7 were calculated from bands [(0, 0), (1, 0), (2, 0), (2, 1), (3, 1), (4, 1), (5, 1), (5, 2)] selected for their intensity and relative freedom of blends with other bands. A similar comparison with the results of Refs. (3, 4, 7, 8) was not possible due to lack of data. The rates due to SRIVASTAVA and MIRZA[3] (Col. 8) correlate very poorly.

The present measurements at low pressures are clearly not applicable for the computation of excitation cross-sections, due to the complexity and magnitude of the deactivation coefficient. We must therefore rely on the measurements at pressures above $P = 2\,\mu$ where ϕ is a well defined quantity. The cross-sections estimated here thus depend on the combined measurements of $I_{v'v''}$ and ϕ. The present estimates of the excitation cross-sections at $E = 100$ eV are given in Col. 10 of Table 3. The greatest uncertainty in the determination of these values arises in the uncertain values of the natural lifetime of the $A\,^2\Pi_u$ state. The cross-sections were calculated using the transition probabilities given by Part I, which were placed on an absolute scale through the lifetime measurements of Ref. (14). The reason for this choice will be discussed in detail in the following section. The argument is essentially that the apparent dominance of heterogeneous deactivation at low pressures results in a lower limit estimate of the lifetime. Thus the higher lifetime obtained by Ref. (14) is considered closer to the real value. There is some evidence that the Ref. (14) results may not be far wrong; the Stern–Volmer plots suggest that heterogeneous deactivation may not have been as severe in their case. In addition the Ref. (14) relative lifetimes of the $A\,^2\Pi_u v = 0, 1, 2$ levels appear not to be greatly diluted by deactivation, since there is good agreement with the relative values determined by the transition probability measurements of Part I. One other lifetime estimate, by HOLLSTEIN *et al.*,[15] $\sim 12\,\mu$sec, based on time of flight measurements was too large to be compatible with the present measurements (see below). The total cross-section as given in Col. 10 (1.2×10^{-16} cm^2, $E = 100$ eV) is thus considered to be a lower limit to the real value. The smallest correction factor for radiationless deactivation determined by the ratio ϕ_v/A_v was about 1.7, at $P = 2\,\mu$. The cross-sections given here are between factors of 2–6 larger than the previous estimates (Refs. 3, 2, 4, 7, 8). None of these earlier estimates were accompanied by lifetime measurements, but were based on the determination of steady state first order dependence on $[N_2]$ and F_e. The total excitation function is given in Fig. 10. Curve (1) is the total cross-section for the production of N_2^+, determined from the total ionization measurements by RAPP and ENGLANDER-GOLDEN,[17] and estimates of the cross-section for production of N^+. The main uncertainty is in the N^+ cross-section, which may be underestimated (cf. KIEFFER and DUNN[32]). Curve (2) is the

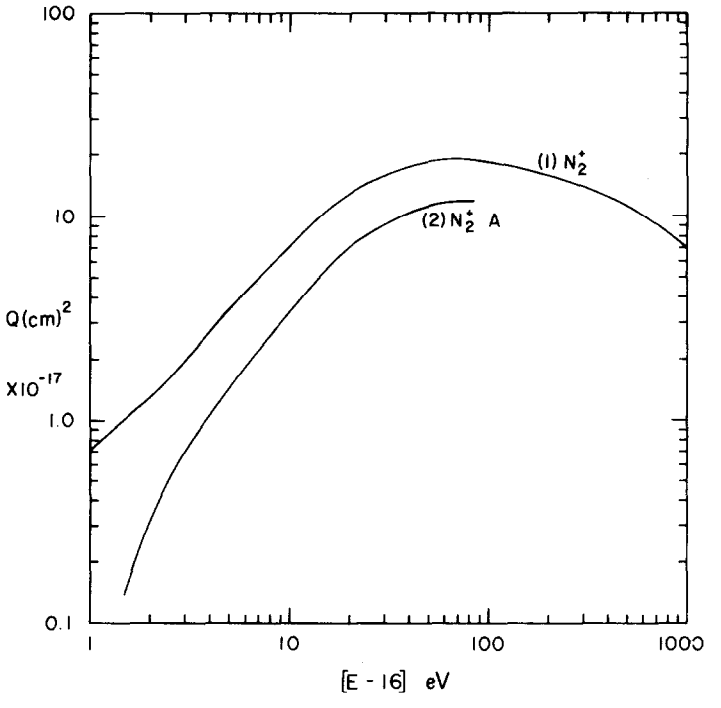

FIG. 10. Excitation functions of the N_2^+ and $N_2^+A\ ^2\Pi_u$. (1) $Q, N_2+e \rightarrow N_2^+ + 2e$. (2) $QA, N_2+e \rightarrow N_2^+A+2e$.

present estimate for production of N_2^+A molecules. Thus at $E = 100$ eV the N_2^+A cross-section is at least 60 per cent of the total N_2^+ cross-section.

Another method of determining the $A\ ^2\Pi_u$ cross-section arises in the apparent well defined nature of all of the ionization cross-sections near threshold. Both the $A\ ^2\Pi_u$ and the $B\ ^2\Sigma_u^+$ are linear in E up to at least 30 eV, and according to Fox[16] and Ref. (17), the total ionization cross-section is also linear between 19 eV–30 eV. The known threshold energies of the three contributing states ($A\ ^2\Pi_u$, $B\ ^2\Sigma_u^+$, $X\ ^2\Sigma_g^+$) should then allow the separation of these same levels from an accurate measure of the total cross-section. The combined measurements of Refs. (16, 17) provide the accurate total cross-section (Fig. 11). The measurements by Ref. (16) were not on an absolute scale, but were made at very high resolution in energy through a retarding potential difference (RPD) method. Curve (1) of Fig. 11 shows the Ref. (16) measurements placed on an absolute scale by the lower resolution Ref. (17) measurements. The smooth line of curve (1) represents the Ref. (17) measurements and the circled points are due to Ref. (16). The two sets of measurements are obviously in excellent agreement. The earlier very low resolution work by TATE and SMITH[33] also shown in the figure, does not correspond well with the Fox measurements. Curve (2) is the present cross-section estimate of the $A\ ^2\Pi_u$ state. The apparent non-linearity in this curve below 18.5 eV is due to the differences in threshold energy of the contributing vibrational levels. Curve (3) is the cross-section for the $B\ ^2\Sigma_u^+$ state, due to Ref. (21). Unfortunately a direct estimate of the $X\ ^2\Sigma_g^+$ cross-section from the slope of curve (1) in the 15.5 eV–16.8 eV region would be very uncertain, due to what Fox suggests may be pre-ionization in

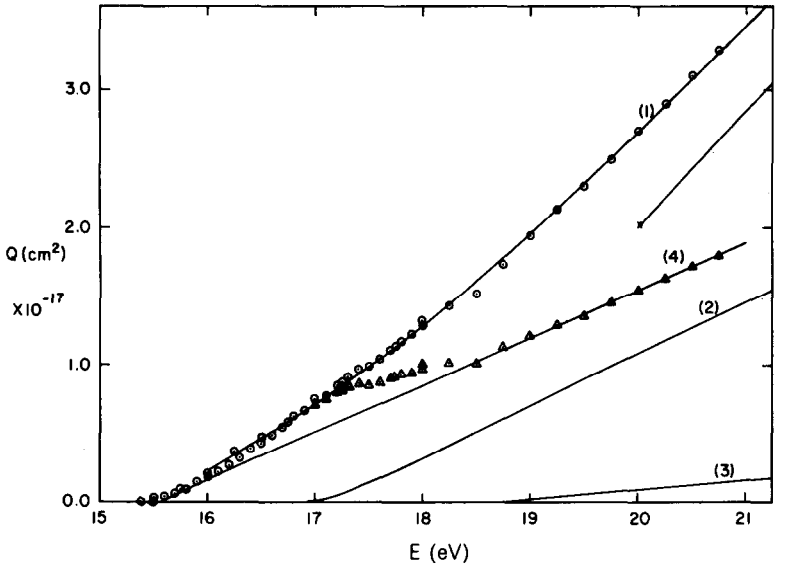

FIG. 11. N_2 ionization cross-sections near threshold. (1) N_2^+, FOX,[16] RAPP and ENGLANDER-GOLDEN,[17] slope $\theta = 7.5 \times 10^{-18}$ cm^2/eV. (2) $N_2^+ A\,^2\Pi_u$, Present work, slope $\theta A = 3.8 \times 10^{-18}$ cm^2/eV. (3) $N_2^+ B\,^3\Sigma_u^+$, ZIPF and BORST,[21] slope $\theta B = 0.65 \times 10^{-18}$ cm^2/eV. (4) (1)$-${(2)+(3)}, $N_2^+ X\,^2\Sigma_g^+$, slope $\theta X = 3.5 \times 10^{-18}$ cm^3/eV. $\odot$ = FOX.[16] $\triangle$ = (1)$-${(2)+(3)}. $\times$ = TATE and SMITH.[33] Best fit to $Q(N_2^+)$ is $\theta A = 3.1 \times 10^{-18}$ cm^2/eV. $\theta X = 3.7 \times 10^{-18}$ cm^2/eV.

the 16.25 eV–18.25 eV region. This deviation from linearity has been observed elsewhere, notably by SCHOEN[18] in a photoionization experiment. However, one can calculate the slopes of the $A\,^2\Pi_u$ and $X\,^2\Sigma_g^+$ excitation functions using curves (1) and (3) in the $E > 18.5$ eV region, through the known threshold energies. This gives a slope (ΘA) for the $A\,^2\Pi_u$ state of 3.1×10^{-18} cm^2/eV, compared to the present lower limit estimate of $\Theta A = 3.8 \times 10^{-18}$ cm^2/eV (curve 2). This is considered good agreement in view of the inaccuracy that can develop in the former method. The compatibility of the present estimate of the $A\,^2\Pi_u$ cross-section with the measured N_2^+ cross-section is illustrated in Fig. 11; the triangled points are the normalized Fox measurements minus curves (2) and (3). The straight line (curve 4) drawn from the $X\,^2\Sigma_g^+$ threshold fits the points rather well, with a slope of $\Theta X = 3.5 \times 10^{-18}$ cm^2/eV. The threshold measurements of the total ionization cross-section thus suggest that the present lower limit estimate of QA is not far from the real value. The present value of ΘA is in fact larger than the value obtained from the total ionization measurement.

5. DISCUSSION

The magnitudes of a number of the measured quantities given in the previous section for the $N_2 1PG$ and $N_2^+ M$ systems are not in agreement with the other recently published results. In our opinion the divergence of the various measurements is due mostly to the assumption that the excitation processes are primary in those regions of current and pressure where linearity with emission rates is obtained. This may not be a sufficient criterion. The higher vibrational levels of the $N_2 1PG$ display a barely detectable variation in emission

rate relative to the lower levels at pressures above $P = 3\ \mu$. However at lower pressures the relative emission rates take on an abrupt linear dependence on pressure, indicating the presence of an afterglow. The afterglow could easily have been overlooked in the higher pressure region due to the apparent first order dependence on $[N_2]$. Our interpretation of the measurements leads to the conclusion that the precursor must be molecules in the $A\ ^3\Sigma_u^+$ state. We will show that the pressure turning point from first order to quadratic dependence depends on the dimensions and, to some degree, the material of the container. The deceptive first order dependence is due to the fact that the precursor population is controlled by homogeneous and heterogeneous collisional deactivation rather than by the radiative lifetime. The N_2^+M system is deceptive in a similar way since the observations can indicate apparently normal Stern–Volmer plots, at least down to a fairly well defined point in pressure, but still give erroneous excitation cross-sections on extrapolation to zero pressure. This is apparent in the present experiment in which the lifetime measurements indicate a maximum lifetime in the region of $P = 2\ \mu$ and a non-exponential decay at lower pressures. The interpretation of this behavior is again based on diffusion, in an electric field in this case, which loses its pressure dependence at low pressures due to heterogeneous collisional deactivation.

The differences with the earlier work may thus arise, to a good degree, in the interpretation rather than in instrumental difficulties. The following discussion of the measurements will therefore be more detailed than would ordinarily be the case.

A. The $N_2 1P$ system afterglow

The possibility that the excitation of the $N_2 1PG$ in an electronic discharge in low pressure N_2 may not be largely due to direct excitation and cascade from the $C\ ^3\Pi_u$ state, arises most obviously in the lifetime measurements of JEUNEHOMME.[9] His observations, in the pressure region where cross-section measurements are generally made, indicated more than one damping constant in the decay of all of the vibrational levels ($v' = 0$–10). The processes not associated with the natural decay contributed more than 50 per cent of the observed emission in pure N_2. Moreover, the damping constants (5.6×10^4, $2.4 \times 10^4\ \text{sec}^{-1}$) and the associated contributions to the emission did not vary greatly with pressure, in the $4 \rightarrow 40\ \mu$ region, or with v'. WENTINK *et al.*[30] reported a similar result using a pulsed electrodeless discharge in a similar arrangement to that of Jeunehomme. The additional sources are much more likely to be due to an afterglow process than to spontaneous emission from higher states, because the uniformity of the contributions to the populations of the vibrational levels tends to rule out the possible cascade transitions (cf. Ref. 30). The source of the afterglow is not obvious, and will be discussed later, in the context of the present measurements. However, the feature to be noted at this point is that the process would not be distinguishable from direct electron excitation without a lifetime measurement, because of the linearity of emission rate with respect to electron flux, and N_2 pressure. Thus it is possible that electron cross-section estimates of the $N_2 1PG$[2,1,7,8] made without regard to the lifetime of the emission, could be in error due to secondary processes of this kind. Differences in vibrational distribution suggest that the very similar effects observed by Jeunehomme and Wentink *et al.* may not be directly related to the afterglow described in the previous section. However, there is one common aspect of the two sets of measurements; the fractional contribution of the secondary process displays very little pressure dependence above $P = 3\ \mu$.

The enhancement of the $v' = 6$–12 levels of the $B\,^3\Pi_g$ state (cf. Fig. 4) at pressures above $P = 0.5\,\mu$ immediately suggests the possibility that the afterglow source is related to that of the L–R afterglow observed at higher pressures. The major difference between the two cases is the absence of N in any significant quantity in the electron gun due to the use of research grade N_2, whereas the L–R afterglow proper is characterized by a well defined dependence on ground state N. However the recombination of $N(^4S)$ does not correspond to the $B\,^3\Pi_g$ state and an intermediate step in the process is required. The precursor or precursors to the $B\,^3\Pi_g$ state have been the subject of controversy, but the latest and possibly most convincing argument has been presented for the $A\,^3\Sigma_u^+$ state (CAMPBELL and THRUSH[34]). The fact that the afterglow contribution observed in the present experiment appears to be almost independent of the energy of the exciting electrons, restricts the possible precursors to molecules in the $A\,^3\Sigma_u^+$ state. The effective production rate of the precursor must clearly follow the excitation function of the $B\,^3\Pi_g$ state. Electrons at $E = 11.5$ eV can excite only the $B\,^3\Pi_g$ and $A\,^3\Sigma_u^+$ states with a significant degree of efficiency. Moreover the $A\,^3\Sigma_u^+$ is the only state with an excitation function known to be both similar in shape and aligned closely enough in energy (cf. WILLIAMS and DOERING,[35] FREUND[36]) to the $B\,^3\Pi_g$ state function, to account for the energy independence of the fractional contribution of the afterglow. The other states in the appropriate energy region ($^3\Delta_u$, $B'\,^3\Sigma_u^-$) with unknown excitation functions are very poor prospects. The $^3\Delta_u$ state has never been observed, and does not appear in the recent electron energy loss spectra at any scattering angle. The ($B'\,^3\Sigma_u^- - B\,^3\Pi_g$) transition is allowed, but is not present in any of the low pressure spectra observed here, or in the energy loss spectra. This system is readily observed, blended with the $N_2 1PG$, in afterglow spectra at higher pressures. The potential energy curves of the $A\,^3\Sigma_u^+$ and $B\,^3\Pi_g$ states are closely aligned and cross near $B\,^3\Pi_g v = 6$ (GILMORE[37]). Thus it seems certain that the second order dependence on $[N_2]$ in the $P = 0.5\,\mu$–$2\,\mu$ region must be due to collisional transfer from N_2A $v > 6$ to the N_2B levels. The tendency toward a first order dependence on $[N_2]$ at pressures greater than $P = 2\,\mu$ can be explained in terms of a transition in dominance from heterogeneous to homogeneous deactivation of N_2A molecules.

Our interpretation of the observations thus indicates that the following reactions control the N_2B and N_2A populations:

$$N_2 + e \rightarrow (N_2B, N_2A) + e \tag{1'}$$

$$N_2A + N_2 \rightarrow N_2B + N_2 \tag{1}$$

$$N_2B + N_2 \rightarrow N_2^* + N_2^{**} \tag{2}$$

$$N_2A + N_2 \rightarrow N_2^* + N_2^{**} \tag{3}$$

$$N_2A + \text{surface} \rightarrow N_2. \tag{8}$$

We do not consider the reaction

$$N_2A \rightarrow N_2B + h\nu$$

a possible contributor to the observed vibrational development of the $B\,^3\Pi_g$ $v > 4$ levels. There is no experimental evidence for the transition; the observed afterglow second order dependence on $[N_2]$ in the laboratory is not compatible with a precursor having a population controlled by spontaneous emission. A significantly large natural damping factor

would be most obvious in the high altitude auroral measurements. However, as we have noted, the auroral observations show a lower vibrational development than the laboratory measurements. The $A\,^3\Sigma_u^+ - B\,^3\Pi_g$ transition must take place over approximately the same region of internuclear distance as does the $B\,^3\Pi_g - A\,^3\Sigma_u^+$ transition. The effective value of the electronic transition moment for a given v''-progression in the $A\,^3\Sigma_u^+ - B\,^3\Pi_g$ system would therefore be of the same order as the values for the $N_2 1P$ system. But the very small v^3 and Franck–Condon factors (cf. BENESCH *et al.*[26]) associated with the former system could easily make the natural damping factor 10^6 smaller than that of the $N_2 1PG$. Thus the natural lifetimes of the higher vibrational levels of the $A\,^3\Sigma_u^+$ state are probably determined by the $A\,^3\Sigma_u^+ - X\,^1\Sigma_g^+$ transition, just as they are for the lower levels.

The intensity of a given v''-progression in the $N_2 1PG$ (IB_v) is then given by the relation

$$IB_{v'} = F_e(QB_{v'})[N_2]\left[\frac{AB_{v'}}{AB_{v'} + [N_2]k_2 v'}\right]\left[1 + \frac{(QA_{v'}/QB_{v'})[N_2]k_1 v'}{k_8 + [N_2]k_3 v'}\right] \tag{8}$$

where F_e is electron flux, QB_v, QA_v, AB_v, AA_v are electron excitation cross-sections and transition probabilities of the $B\,^3\Pi_g$ and $A\,^3\Sigma_u^+$ states, respectively, and $k_i v$ is the rate coefficient for reaction i. We compare these levels of the $B\,^3\Pi_g$ state with the $v' = 4$ level which, along with the $v' = 3$ level, is first order in $[N_2]$ and has a single, well defined lifetime at least up to pressures of $P = 10\,\mu$. Thus we have

$$\frac{IB_{v'}}{IB_4} = \left(\frac{QB_{v'}}{QB_4}\right)\frac{AB_{v'}(AB_4 + [N_2]k_2 4)}{AB_4(AB_{v'} + [N_2]k_2 v')}\left[1 + \frac{(QA_{v'}/QB_{v'})[N_2]k_1 v'}{k_8 + [N_2]k_3 v'}\right]. \tag{9}$$

The natural lifetime of the $A\,^3\Sigma_u^+$ state[38–40] is too long to have a significant effect on the population and the lifetime is determined entirely by the term $(k_8 + [N_2]k_3 v')$. Absolute values of the cross-sections for reaction (1′) are not necessary in this case. The relative values have not been accurately determined but the most reliable estimates (QB, QA) presently arise from electron energy loss spectra (Ref. 35, BRINKMANN and TRAJMAR[41]). The spectra are of high enough resolution to separate vibrational levels, but high background counts and blending of levels of different states make quantitative measurements difficult. FREUND[36] has made an estimate of (QB/QA) from measurements of the total excitation function, but these depend on the ratio (QB/QC) and separation of poorly resolved excitation functions. However, the evidence as a whole does seem to indicate a large QA about the same magnitude as QB, and relative vibrational population rates roughly conforming to the Franck–Condon factors for the excitation transition ($A\,^3\Sigma_u^+ - X\,^1\Sigma_g^+$). Reaction (2) is not important in this particular case, but is included for completeness since it is dominant in the L–R afterglow at higher pressures. The variation of ($IB_{v'}/IB_4$) thus depends essentially on the relative values of k_1, k_3 and the variation of k_8. At the high pressure end of the measurements, ($IB_{v'}/IB_4$) approaches independence of $[N_2]$, and the ratio $(QA_{v'}/QB_{v'})\,k_1 v'/k_3 v'$ is determined by ($QB_{v'}/QB_4$). We take the ratio of the Franck–Condon factors ($B\,^3\Pi_g - X\,^1\Sigma_g^+$) as the value of ($QB_{v'}/QB_4$) since the auroral measurements suggest a high correlation with the theoretical rates, and the laboratory measurements at $P = 0.5\,\mu$ tend to approach these values. The absolute values of $(QA_{v'}/QB_{v'})\,k_1 v'$ and $k_3 v'$ are determined at the low pressure end of the measurements where the lifetime term $(k_8 + [N_2]k_3)$ of the $A\,^3\Sigma_u^+$ state is determined by k_8. The uncertainty in the estimate of $k_1 v'$ and $k_3 v'$ arises mostly in the estimation

of k_8. The effective diffusion length is difficult to estimate theoretically due to the complexity of shapes and variety of surfaces in the electron gun. However, the value of k_8 tends to be independent of $[N_2]$ in the $P = 0.5\ \mu$ region since the mean free path is longer than the distance to the surfaces. Thus we apply an upper limit to k_8 at $P = 0.5\ \mu$ on the basis of average flight time to the surface. The effective radius of the container is then determined by the pressure dependence that k_8 must display in order to fit the observations (See Appendix). The effective radius of the container for fundamental mode diffusion to the walls, required for a good fit to the data, is roughly four times the geometric radius. This suggests that the container walls are not very efficient as deactivators of N_2A molecules. More direct evidence for a resistance to heterogeneous deactivation of $[N_2A]$ (by glass) arises in the NOXON[42] high pressure afterglow experiment; the decay rate of $[N_2A]$ at 760 Torr in this experiment places a well defined limit on loss due to diffusion, and requires an effective radius several times larger than the geometric value (SHEMANSKY[43]). There is also some evidence for a resistance to deactivation by metallic surfaces. WEINREB and MANELLA[44] present measurements of the production of N_2B by surface-catalyzed recombination of N in a metallic sieve (nickel, silver), implying production of N_2A at the metallic surface.

The calculated curves (equation 9) and experimental points for the $v' = 6, 11$ levels are shown in Fig. 5. Rate coefficients for reaction (3) for the corresponding N_2A state levels are given in Table 4. The variation of $[N_2A]$ deactivation rate is shown in Fig. 5. The accuracy

TABLE 4. AFTERGLOW RATE COEFFICENTS AND DATA

1	2	3	4	5	6	7	8	9	10
$v(A\ ^3\Sigma_u^+)$	$v(B\ ^3\Pi_g)$	k_3v	$\left(\frac{QA_v}{QB_v}\right)k_1v$	k_1v/k_3v^a	$\Delta(ev)^b$	$\frac{QA_v^a}{QB_v}$	gBv^c	gBv^d	gBv^e
7	0				7.9–3	2.2		44	61
9	1				−8.3–2	0.94		27	24
10	2				−2.2–2	0.65		40	25
11	3				4.0–2	0.60		23	25
13	4				−4.3–2	0.54		12	18
14	5	6–11	8–12	0.2	2.3–2	0.65	7	10	22
16	6	3.7–11	1.5–11	0.60	−3.3–2	0.66	22	15	15
17	7	1.4–10	6.6–11	0.54	3.7–2	0.87	19	4.1	19
19	8	7–10	5–10	0.8	−2.6–3	0.91	10	3.3	7
21	9	5–10	5–10	1.0	−2.9–2	1.0	9	2.6	7
22 23	10	3.1–10	6.4–10	0.86	5.2–2 −4.0–2	2.4	7	10	8
24 25	11	2.2–11	1.0–10	1.8	4.6–2 −3.7–2	2.6	9	35	12
26 27	12	6–11	6–10	3.7	5.6–2 −1.7–2	2.6	12	16	
							$\sum_{v=5}^{12} g_v = 96$		

[a] Based on analytic function for $QA_v \propto q_{v,0} = (1.90)(10^{-4})(v+1)^{4.74} \exp -0.527\,v$ as an extrapolation beyond $v = 13$.
[b] $\Delta = (EB_v - EA_v)$.
[c] Relative population rates of $B\ ^3\Pi_g$ due to afterglow in present work.
[d] Relative population rates of $B\ ^3\Pi_g$ due to L–R afterglow.
[e] Relative population rates of $B\ ^3\Pi_g$ due to JEUNEHOMME[9] experiment.

of the relative values of $k_3 v$ is variable. Levels $B\,^3\Pi_g v = 7, 8, 9$ are rather uncertain because they do not display the well defined variation observed in the $v = 6$, 10, 11, 12 levels. A crude estimate of the relative rates of reactions 1 and 3 is given in Table 4, Col. 5. These values are determined by assuming the relative cross-sections (QA_v/QB_v) proportional to the Franck–Condon factors for the ground state transitions, and $QA = 1.5\,QB$. Franck–Condon factors $(q_{v',0})$ for the transition $(A\,^3\Sigma_u^+ - X\,^1\Sigma_g^+)$ are available only up to $v' = 13$ (BENESCH *et al.*[26]), and an analytic approximation (Table 4) was used to make a crude extrapolation. This is reasonable in this case since the $q_{v',0}$ factors are a smoothly varying function of v'. The approximation gives an accurate fit to the Benesch *et al.* numbers beyond $v' = 1$, and obeys the sum rule $\Sigma_{v'} q_{v',0} = 1$. Note that the levels $B\,^3\Pi_g v = 11, 12$, which we assume are supplied by two $A\,^3\Sigma_u^+$ levels, have estimated ratios $(k_1 v/k_3 v) > 1$, an impossibility. Order of magnitude errors in the estimated relative (QA_v/QB_v) values for the $A\,^3\Sigma_u^+ v = 24$–27 levels would not be surprising. It is also possible that vibrational deactivation of the levels just below the dissociation limit may go at a high rate, and hence tend to raise the effective QA_{24-27}. It is noteworthy that there is a very good correspondence of the magnitude of the energy difference between vibrational levels of the two states, $\Delta(=EB_v - EA_v)$, with the magnitudes of $k_3 v$ with the exception of the three values k_3 17, 21, (22, 23). The correspondence of Δ with $k_1 v$ is not as good. Cols. 8 and 9 of Table 4 give the relative population rates of the $B\,^3\Pi_g$ state due to the afterglow in the present observations, and due to the L–R afterglow, calculated from the BAYES and KISTIAKOWSKY[45] measurements. There is a surprising correspondence in the relative intensities of the $v' = 5, 6$, and 12 levels, in view of the different excitation mechanisms of the $A\,^3\Sigma_u^+$ state in the two cases. If we assume that production of $B\,^3\Pi_g v = 5$–12 molecules is due entirely to reaction (1) in the L–R afterglow, the emission rates from the v' levels depend on the relative rates of reactions (1) and (3), and of (2) and the recombination rate of N (SHEMANSKY[43]). The rate coefficients of reaction (2) are not available for all of the vibrational levels. Jeunehomme presents data indicating the pressure dependence of lifetime for the case of a 10:1, $NO:N_2$ mixture, and the rate coefficients would not necessarily be representative of pure N_2. Active O, for example, is known to have a profound effect on the $B\,^3\Pi_g v = 6$ level (cf. OLDMAN and BROIDA[46]). Earlier less accurate measurements presented by JEUNEHOMME and DUNCAN[47] in pure N_2 may also be invalid, since the presence of multiple damping constants was not recognized at that time. These measurements indicate a variation in deactivation coefficients from 0.8×10^{-11} cm^3/sec for $v' = 12$ to 6.5×10^{-11} cm^3/sec for $v' = 5$. The rates, measured in the 1 Torr region, could easily be influenced to varying degrees by the afterglow process. FOWLER *et al.*[48] present measurements in the $P = 50\,\mu$ region which suggest very little variation in deactivation rate over the $v' = 5$–8 levels, with values in the region of 3×10^{-11} cm^3/sec. However the accuracy of the estimated rate is again uncertain for the same reason cited for the Jeunehomme and Duncan measurements. We give more weight to the relative values of the lower pressure measurements of Fowler *et al.* and for the purpose of the present calculation assume that k_2 does not vary with v'. The value $k_2 3 = 7.6 \times 10^{-11}$ cm^3/sec measured in the present work has been adopted, since it is probably the most accurate among available data. The observed population rates clearly do not correspond to the trend in the $k_1 v/k_3 v$ ratio estimated in Table 4. This combination of $k_1 v/k_3 v$ and k_2 thus requires resonance in the recombination rate of N at $A\,^3\Sigma_u^+ v = 5, 6$, and 11 in order to fit the observed intensities. The absence of an afterglow effect in our observations of the $B\,^3\Pi_g v = 3, 4$ levels at $P = 10\,\mu$

and below does not represent a discrepancy with the L–R afterglow observations, since the populations of these levels are due entirely to the ($B'\,^3\Sigma_u^- - B\,^3\Pi_g$) transition in the latter case. This transition also contributes measurably to the $B\,^3\Pi_g v = 2, 5$ levels, but contributions to the levels 0, 1 are unknown since they depend on the unobserved near infrared radiation from the lower vibrational levels of the $B'\,^3\Sigma_u^-$ state. The radiative transitions $B\,^3\Pi_g - A\,^3\Sigma_u^+ v = 7, 9, 10$ combined with reaction (1) may contribute about one-half the population rate gB_0 and lesser fractions of gB_1 and gB_2. Afterglow contributions to the $B\,^3\Pi_g v = 1, 2$ levels are not detectable in the present experiment because of the relatively large electron cross-sections of these levels and variable contributions from the $C\,^3\Pi_u$ state. There is some inconsistent evidence for a variation of relative IB_2 with pressure. An afterglow contribution of the order of the contribution to the $B\,^3\Pi_g v' = 12$ level could go undetected in these levels. The quantitative estimate of the relationship of $I1PG$ and $[N]^2$ by Campbell and Thrush combined with the rate coefficients determined here allow an estimate of the rate coefficient for the production of N_2A molecules by recombination of N. This amounts to a substantial fraction of the total recombination rate and has been shown to be compatible both in magnitude and dynamically with the L–R afterglow (SHEMANSKY[43]).

We wish to emphasize that the magnitudes and some of the relative values of the rate coefficients given in Table 4 are crude estimates. The major source of error for $k_3 v$ is in the estimation of k_8. Unfortunately lifetime measurements of the $B\,^3\Pi_g$ levels most affected by the afterglow were not made. However it was possible to place upper and lower bounds to the value of k_8 (Appendix), and the two figure numbers are considered accurate to within a factor of 2 or 3. The one figure numbers have a greater uncertainty since the associated levels did not have an easily measured variation in relative intensity at the lower pressures, but must have values an order of magnitude larger than the others in order to be compatible with the observations. We assume that k_8 is independent of v.

The ratio $QA/QB = 1.5$ used in the calculations is an estimate obtained from the Williams and Doering electron energy loss spectra. Brinkmann and Trajmar obtain a value $QA/QB = 1$. A much larger value of QA/QB would be incompatible with the L–R afterglow. The general trend of the effective QA_v/QB_v as a function of v, whatever the absolute values may be, is unlikely to be much different from that given in Col. 7 of Table 4. Sources other than direct electron excitation of the $A\,^3\Sigma_u^+ v > 13$ levels, with the possible exception of vibrational cascade in the highest levels, should be negligible; transitions from $B\,^3\Pi_g$ affect only the levels with $v < 13$, and the amount of N present especially at low electron energies would be far too low to produce a significant recombination rate. Although the variation of reaction (2) for all v' is not well determined, the FOWLER *et al.*[48] data indicates little change over the levels in question here, $v' = 5$–8. The present measurements also suggest that there could be no very large individual values of $k_2 v$. There is therefore a strong suggestion that the three body recombination of N must have a resonance at the $A\,^3\Sigma_u^+ v = 14, 16$ levels, if the proposed process for the L–R afterglow is valid. The intensity distribution in the $N_2$1P system and the lack of significant variation with pressure tend to rule out redistribution of population by vibrational deactivation in either of the ($A\,^3\Sigma_u^+, B\,^3\Pi_g$) states; electronic deactivation rates in the relevant levels are evidently at least an order of magnitude greater than the corresponding vibrational rates, with the possible exception of the highest vibrational levels of the $A\,^3\Sigma_u^+$ state. Selective deactivation by N seems unlikely over a group of three consecutive vibrational levels. There is a strong

suggestion that deactivation of $A\,^3\Sigma_u^+ v = 0, 1$ by N is 2–3 orders of magnitude less than has been previously estimated (SHEMANSKY,[43] cf. THRUSH[49]). This would make reaction (2) dominant if the rate for N also applied to the higher vibrational levels.

It is clear that the afterglow in the $N_2\,1P$ system observed in the present experiment would be difficult to avoid in any electron gun experiment designed to measure excitation cross-sections. The various measurements of relative population rates should differ only in degree, depending on the dimensions of the container and the efficiency of the heterogeneous deactivation. The STANTON and ST. JOHN[2] measurements indicate relative rates intermediate between the extremes of the present observations, and are doubtless affected by the same processes. The MCCONKEY and SIMPSON[1] measurements also have a distribution with a greater vibrational development than expected for electron excitation, but with a less exaggerated divergence. However, as previously mentioned, these (Ref. 1) results are not very consistent with respect to the relative transition probabilities for a given upper state level, and the relative rates depend on the particular bands chosen for the calculation. A comparison of the various measurements of absolute electron excitation cross-sections (QB_v) must therefore be restricted to the levels $v < 5$ in order to avoid the afterglow as much as possible. The discrepancies between the present and earlier measurements in the $v < 5$ levels are thus assumed to have some other source, such as the geometric considerations already discussed in the previous sections.

The Jeunehomme experiment cannot be readily explained in terms of the results of the present work. The relative population rates of the $B\,^3\Pi_g$ state in that experiment (Col. 10, Table 4) bear no resemblance to the distribution due to electron impact, and in fact, correlate rather well with a combination of the distribution of the afterglow measured in the present work and the L–R afterglow (Cols. 8, 9, Table 4). No combination of distribution due to electron excitation and L–R afterglow correlates with the Jeunehomme observations. The apparent lack of significant variation, due to the precursor, of both the fractional contributions to the volume emission rates and the lifetimes, as a function of pressure, tends to rule out any simple afterglow process such as the one observed in the present experiment. Reactions (1′, 1, 2, 3, 8) must contribute to some degree to the control of the $B\,^3\Pi_g$ state populations, but other processes are obviously taking part. Both the Jeunehomme, and Jeunehomme and Duncan experiments would almost certainly produce much more N than the present case, due to the presence of NO (Ref. 9) and trace impurities (Ref. 47). Transitions from the $B'\,^3\Sigma_u^-$ may contribute to the populations of some of the levels, as they do in the L–R afterglow. The mode of excitation of this state in the afterglow is not known. There is no indication of the presence of $(B'\,^3\Sigma_u^- - B\,^3\Pi_g)$ transitions in the spectra of the present experiment. However, the lifetime measurements of the $B\,^3\Pi_g v = 3$ level at $P = 50\,\mu$ indicates a secondary decay that appears not to be related to the afterglow observed in the higher levels, since it displays an apparent quadratic or higher order dependence on $[N_2]$, and is not detectable at $9\,\mu$ (cf. Fig. 3). The damping constant ($5.0 \times 10^4\ \text{sec}^{-1}$) is about the same as the major secondary component in the Jeunehomme experiment. If the $B'\,^3\Sigma_u^-$ state is indeed the source of the secondary decay in his experiment, the excitation mechanism must not prevail in the electron gun experiments. This suggests that the production of $B'\,^3\Sigma_u^-$ molecules would have to arise in a mechanism such as another branch in the recombination of N. But at these pressures the recombination would necessarily be a catalyzed heterogeneous reaction in order to obtain the required rates, and in order to be compatible with the observed pressure dependence.

In any case cascade from the $B'\,^3\Sigma_u^-$ state alone could not account for the uniform contributions to the $B\,^3\Pi_g$ levels. The secondary decays of most levels would have to be artificial, in the form of blends of bands of the two systems. It is clear there is no very satisfactory explanation of the Jeunehomme experiment.

B. The N_2^+ meinel system

As we have shown in the previous section, the reciprocal Stern–Volmer quenching factor for the N_2^+M bands represented by the plots of Fig. 7, has an apparently normal linear dependence on pressure down to the $P = 1$–$2\,\mu$ region where there is an abrupt change in curvature. If one ignores the resonance in this curve at lower pressures, the tendency of the volume emission rate towards a first order dependence on $[N_2]$ is reminiscent of the variation of the damping term $k_8 + [N_2]k_3$ (Fig. 5) for the $[N_2A]$ molecule discussed in sub-section *A* above. But the lifetime of the $A\,^2\Pi_u$ state is of the same order of magnitude as that of the $B\,^3\Pi_g$ state and one would not expect random diffusion to affect cross-section or lifetime measurements significantly even at the lowest pressures. In any case we observe a non-exponential decay in lifetime of the $A\,^2\Pi_u$ state below $P = 2\,\mu$ which would not be characteristic of random diffusion. However diffusion due to drift is a distinct possibility since an electric field is difficult to avoid as a result of differential diffusion of electrons and ions. At $P = 2\,\mu$ the mean free path is of the order of the radius of the container. The diffusion rate coefficient would thus tend to be time dependent and give rise to a similar dependence in the damping term controlling the decay of the excited molecules. We propose a damping term (ϕ) of the following form, as at least a partial explanation of the observations

$$\phi = A_v + \frac{\bar{v}_D}{L'[N_2] + L} + [N_2]k \tag{10}$$

where k is the rate coefficient for collisional deactivation, and the factor $v_D/\{L'[N_2]+L\}$ represents the loss rate probability due to diffusion. The diffusion loss term is similar in form to that of reaction (8), discussed in the Appendix, but its variation is much more difficult to define in this case. The average drift velocity ($\bar{v}_D$) and the transport lengths L', L depend on the electric and columnating magnetic fields (cf. HASTED[50]). The electric field has an unknown dependence on pressure and electron current. The collisional deactivation coefficient (k) may also have a dependence on $\bar{v}_D$.

The reactions represented by Equation (10) appear to be the only reasonable explanation of the observations. The deviation from approximate first order dependence on $[N_2]$ shown in Figs. 7, 8 occurs at pressures in the region where the N_2^+A molecules should be collision free during their lifetimes, if we neglect the presence of the electric and magnetic fields. Homogeneous recombination ($\alpha = 2.5 \times 10^{-7}$ cm^3/sec. KASNER[51]) would be too slow to affect the $A\,^2\Pi_u$ state. The non exponential decay at low pressures, the slight dependence of lifetimes on electron current observed at higher pressures, and the variation of deactivation with electron energy are all consistent with diffusion loss due to drift in an electric field. An extrapolation to zero pressure to determine the natural lifetime is thus very risky due to the complex and ill defined nature of equation (10). The excitation cross-sections presented here are as a consequence subject to the uncertainty in the measured natural lifetime.

Evidence of effects similar to those described here, is present in the earlier published estimates of excitation cross-sections for the two cases wherein measurements are given in sufficient detail. SIMPSON and MCCONKEY[4] show plots of the reciprocal Stern–Volmer quenching factor with a definite dependence on electron energy and a well defined change in curvature at $P = 1.5\,\mu$ similar to that shown in Fig. 7. The authors do not attempt to explain the energy dependence of the quenching factor, but interpret the break in curvature as an onset of collisional deactivation with the assumption that cross-section measurements below $P = 1.5\,\mu$ were valid. In our opinion this is an erroneous interpretation, since it implies an unreasonable pressure dependent deactivation rate coefficient, that in effect drops to zero at pressures in the region of $P = 1.5\,\mu$. The loss of pressure dependence of the effective deactivation coefficient is much more likely to be due to the combination of diffusion and deactivation terms (equation 10). O'NEILL and DAVIDSON[14] also present Stern–Volmer plots with changes in curvature in the $P = 1$–$2\,\mu$ region, but with a less drastic change in slope than in the present and Simpson and McConkey observations. The effect may be somewhat exaggerated in the present Stern–Volmer plots of Fig. 7, since the measurements were made at a constant production rate, and the electron current would be very high in the low pressure region, in comparison with the currents actually used in the cross-section measurements. The lifetime measurements given by Ref. (14) also show a systematic deviation from a linear dependence on pressure. As we have noted in the previous section, the linearly extrapolated lifetimes measured by O'Neill and Davidson are about 1.5 times longer than the extrapolation of the present observations. The published observations of Refs. (2, 3, 7, 8) do not contain enough detail to provide the information contained in the Stern–Volmer plots. It should be emphasized that none of the estimates of excitation cross-sections in the literature, of either the $N_2 1P$ or $N_2^+ M$ systems are accompanied by a discussion of lifetimes in relation to the electron beam diameter; the volume production rate will always be significantly larger than the volume emission rate for these two systems, unless the electron beam diameter is very large. The Stanton and St. John measurements should have some advantage because of the 1 cm diameter electron beam used in their experimental arrangement. This may be reflected in the (factor of 2) larger cross-sections for $N_2^+ M$ obtained by these workers in comparison to the Simpson and McConkey measurements, as opposed to the reasonable agreement of the two groups in the $N_2 1PG$ cross-section estimates. We regard the Srivastava and Mirza measurements as rather uncertain due to the very poor correlation of the relative vibrational population rates with the predicted rates, in comparison with the other measurements.

The tendency for loss rates due to diffusion to increase with decreasing pressure, suggests that the rough linear extrapolation of the damping constant in the present work and by O'Neil and Davidson results in estimates of lower limits of the natural lifetime of the $A\,^2\Pi_u$ state. The smaller effective deactivation coefficients indicated by the lifetime measurements suggest that diffusion was less severe in the latter case. Thus it is not surprising that their extrapolated lifetimes are larger than the present estimates. The cross-section estimates (Table 3) based on the O'Neil and Davidson lifetime measurements are therefore considered lower limits to the real value. The excitation of the $A\,^2\Pi_u$ state must then account for at least 60 per cent of the total ionization cross-section. This corresponds well with measurements of the related process, photoionization (cf. SEATON[52]), by SCHOEN[18] who obtained a ratio $N_2^+ B : N_2^+ A : N_2^+ X \approx 10:60:30$. The lifetime measurements of HOLLSTEIN *et al.*,[15] $\sim 12\,\mu$sec, which should not be subject to the difficulties encountered in the electron gun

experiment, are not compatible with the present measurements since the resulting cross-sections would be equal to the measured total ionization cross-section for the production of N_2^+ (1.9×10^{-16} cm^2, for $E = 100$ eV). The total ionization cross-section is considered to be very well determined,[17,32] and the error must very likely lie in either the present or the HOLLSTEIN *et al.*[15] experiments. There is no obvious reason for error in the latter experiment, since their lifetime measurements of $N_2 1PG$, with the same apparatus used in a different mode, agrees well with the present and Jeunehomme estimates. It may be argued that the present $N_2^+ M$ lifetime measurements possibly would not correspond to the stationary conditions in the electron gun even at higher pressures where the decay is exponential. However, the equality of lifetimes measured on both the rising and falling edges of the gated electron beam is good evidence to the contrary. According to the present measurements an upper limit of about 9 μsec must be placed on the $N_2^+ M$ ($v = 2$) lifetime. Some weight must be given to the threshold measurements of the total ionization cross-section by FOX[16] combined with the absolute measurements of Rapp and Englander-Golden. The compatibility of these two sets of measurements (cf. Fig. 11) and the accuracy claimed by the authors, suggests that the slope of the total ionization cross-section should be in error by less than 10 per cent. This would place the slope of the $A\ ^2\Pi_u$ state between the limits 5×10^{-18} and 2×10^{-18} cm^2/eV, with the most probable value of 3.1×10^{-18} cm^2/eV, in reasonable agreement with the present experiment (3.8×10^{-18} cm^2/eV). The threshold measurements thus tend to support the O'Neil and Davidson lifetime estimates as measures of the natural lifetimes. Further carefully designed experimental measurements of the lifetime are essential.

The dependence of deactivation of $N_2^+ A$ molecules on electron energy and current may well be the cause of disparity among the various measurements of the shape of the excitation function (cf. SIMPSON and MCCONKEY[4]). The uncorrected excitation functions observed in the present experiment with electron current as parameter, take on the same general shapes as those presented in the earlier literature. For example, the Simpson and McConkey shape functions have a resemblance to those obtained here at high currents, in which the threshold region does not have a linear dependence on energy, and the shape as a whole is flattened; the cross-section measurements of Ref. (4) are a factor of 5 lower than the present estimates at 100 eV, but at 20 eV the disparity is reduced to a factor of 2.

6. CONCLUSIONS

A. The $N_2 2PG$

The present estimate of the excitation function of the $N_2 2P(0, 0)$ band agrees well with the earlier work (BURNS *et al.*,[5] JOBE *et al.*[6]) at electron energies $E < 30$ eV. Measurements at higher energies are not in good agreement. This could possibly be due to low energy secondary electrons scattered by the electron gun collector. If this supposition is correct, the measurements by AARTS *et al.*[29] (cf. Fig. 1) in the energy region $E > 50$ eV should be more nearly correct since they are lowest of all the published excitation functions. The Ref. (29) measurements were judged valid since their cross-section measurements of the $N_2^+ 1N(0, 0)$ band in the same spectral region are in good agreement with the generally accepted values. Those measurements which were in good agreement with the experimentally

determined relative transition probabilities of WALLACE and NICHOLLS,[24] TYTE,[25] also indicated good correspondence with the theoretical relative population rates for the excitation transition, $C\,^3\Pi_u - X\,^1\Sigma_g^+$ (Refs. 5, 7, 25). The results presented by Ref. (6) were not compatible with the transition probabilities, and as a result the estimated relative population rates displayed a dependence on the particular bands chosen for the calculation.

The present estimate of the peak excitation cross-section of the (0, 0) band is $QC(0,0) = 1.04 \times 10^{-17}$ cm^2 at $E = 14.7$ eV. The total peak cross-section based on $QC(0,0)$ and the theoretical relative population rates is $QC = 3.8 \times 10^{-17}$ cm^2 (Table 1). This (QC) is in good agreement with Ref. (5), but is a factor of about 1.5 larger than the estimate by Refs. (7, 8). We disregard the value given by Ref. (6) for the reason given above. There is no ready explanation for the disagreement with Refs. (7, 8). Very little information is available for the latter work. However, the present measurements are internally consistent; the ratio QC/QB determined from the relative population rates of the $B\,^3\Pi_g$ state, is in good agreement with the direct measurements of the cross-sections.

B. *The $N_2$1PG*

The excitation of this system by electron impact is complicated by secondary processes, even at the lowest pressures applied in obtaining laboratory spectra. According to the present work $B\,^3\Pi_g v > 4$ levels are affected by an afterglow with an approximate first order dependence on $[N_2]$ down to pressures in the $P = 2$–$3\,\mu$ region, below which a tendency toward second order dependence takes place. Analysis of the observations suggests that the afterglow would be very difficult to avoid in any experimental arrangement. The only variable would be a limited dependence on the size and material of the container. The point in pressure at which the afterglow changed from first to second order dependence would thus vary from one experimental arrangement to another. The two other publications of cross-sections for this system that present enough information to allow calculation of relative population rates[1,2] are consistent with this analysis since they indicate $B\,^3\Pi_g$ population distributions intermediate between the extremes of the present observations. The presence of secondary effects was not recognized in the earlier cross-section work, although such processes have been strongly suspected and recognized elsewhere.[9,11,30] We conclude from the present observations and observations of high altitude weak aurora,[19] that the relative population rates of the $B\,^3\Pi_g$ levels due to direct electron excitation correlate well with the theoretical rates for the $B\,^3\Pi_g - X\,^1\Sigma_g^+$ transition. The cross-sections of the $B\,^3\Pi_g$ levels were determined from measurements of the (3, 1) band; lifetime measurements indicated the $v = 3$ level was not affected by the afterglow at pressures $P < 10\,\mu$, in the present experiment. The excitation function at energies $E < 30$ eV (Fig. 2) as measured in the present work is similar in shape to the functions presented by Refs. (1, 2). The peak cross-section of the (3, 1) band is $QB_{3,1} = 1.15 \times 10^{-17}$ cm^2 at $E = 10.8$ eV. The total peak cross-section of the $B\,^3\Pi_g$ state was estimated to be $QB = 1.2 \times 10^{-16}$ cm^2. Comparison with the earlier measurements was restricted to the lower levels in order to exclude secondary effects as much as possible. Although the shapes of the measured excitation functions are similar, the absolute values of the present functions are factors of 1.4–1.9 larger at the peak than the Ref. (1, 2) results (Table 2). The most plausible explanation for this difference arises in the fact that the latter appear not to have

taken cognizance of the rather long lifetime of the $B\,^3\Pi_g$ state; in electron beam experiments the volume production rate would be measurably greater than the volume emission rate by factors depending on the diameter of the electron beam. Total excitation functions presented by Refs. (7, 8) having peak values $QB = 1.0 \times 10^{-16}$ cm^2 and 1.4×10^{-16} cm^2 were determined using transition probabilities based on a constant electronic transition moment (cf. Part I), and for this reason direct comparison with the present work would serve no purpose. Details of the Ref. (7, 8) measurements were not available.

A measure of the ratio QC/QB has been obtained independently of the direct cross-section measurements by correlating the population rates of the $B\,^3\Pi_g$ state calculated for various fractional contributions from the $C\,^3\Pi_u$ state, with the experimental measurements. The averaged result, $QC/QB = 0.27$ for $E > 17$ eV is in good agreement with the directly measured ratio of the peak cross-sections, $(QC/QB)_{\text{peak}} = 0.32$. The difference between the two ratios is in the direction of the trend in relative shapes of the excitation functions.

We conclude by a process of elimination that molecules in the $A\,^3\Sigma_u^+$ state must be the precursors to the observed low pressure afterglow. The excitation function of the precursor must have a similar shape and must occupy almost the same position on the energy scale, as the $B\,^3\Pi_g$ function. The $A\,^3\Sigma_u^+$ is the only state having these characteristics with a large enough excitation cross-section to explain the observations. Spontaneous emission in the $(A\,^3\Sigma_u^+ - X\,^1\Sigma_g^+)$ system plays a negligible part in the deactivation of the $A\,^3\Sigma_u^+$ state; homogeneous and heterogeneous collisions control the $A\,^3\Sigma_u^+$ population. The population rate of the $B\,^3\Pi_g$ levels through collisional deactivation of the $A\,^3\Sigma_u^+$ levels would thus be first order in $[N_2]$ in the pressure regions where homogeneous collisions control the $A\,^3\Sigma_u^+$ population. At lower pressures where wall collisions dominate $A\,^3\Sigma_u^+$ deactivation, the $B\,^3\Pi_g$ population rate takes on the observed second order dependence on $[N_2]$. Crude estimates of the deactivation rate coefficients for production of $B\,^3\Pi_g$ molecules are in the region of the gas kinetic value (Table 4). The population rate distribution of the $B\,^3\Pi_g$ state due to deactivation of $A\,^3\Sigma_u^+$ molecules has the same general character as the L–R afterglow. Vibrational levels beyond $B\,^3\Pi_g\, v = 12$, corresponding to the dissociation limit for the production of N(^{4}S), are not observed. The $B\,^3\Pi_g v = 3, 4$ levels are not populated at measurable rates by $A\,^3\Sigma_u^+$ deactivation. Although the $v = 3, 4$ levels are populated at substantial relative rates in the L–R afterglow, the source is the $B'\,^3\Sigma_u^- - B\,^3\Pi_g$ radiative transition rather than deactivation of $A\,^3\Sigma_u^+$ molecules. The deactivation coefficients of the $B\,^3\Pi_g$ state ($k_2(3) = 7.6 \times 10^{-11}$ cm^3/sec), although not well determined for all of the levels, along with the coefficients for the $A\,^3\Sigma_u^+$ state appear to be compatible with the magnitudes and dynamics of the L–R afterglow (Ref. 43). It thus seems very likely that the $A\,^3\Sigma_u^+$ state is the major precursor to the L–R afterglow. The vibrational distribution of the combined deactivation coefficients for the $B\,^3\Pi_g$ and $A\,^3\Sigma_u^+$ states suggests that the recombination of $N(^4S)$ must be resonant in the production of $A\,^3\Sigma_u^+$ levels.

The low pressure observations of secondary processes, by Ref. (9) appear not to be directly related to the afterglow obtained here. The population rate distribution in the Ref. (9) work contains a peculiar combination of the rates measured here and those measured in the L–R afterglow. There appears to be no very satisfactory explanation.

The present work is incomplete in that such aspects as rotational population rates due to the afterglow and the peculiar shape of the $B\,^3\Pi_g$ excitation functions near threshold have not been examined in detail. The observations in respect to the afterglow effects are in

fact regarded as preliminary in nature. We have observed no real evidence of cascade from higher states of any significance apart from the $C\,^3\Pi_u - B\,^3\Pi_g$ system.

C. *The N_2^+M System*

It was not possible to make a direct cross-section measurement of this system with the present experimental arrangement due to the relatively long lifetime of the $A\,^2\Pi_u$ state. This is evident in both the steady state and transient measurements, and the combined results suggest that the excited molecules are subject to deactivation due to diffusion or drift in an electric field. We believe this may well be the cause of disagreement among the earlier cross-section work (Refs. 2–4, 7, 8).

Measurements of the Stern–Volmer factor reveal an independence of pressure in the low pressure region that can be reasonably interpreted only in terms of a substantial heterogeneous deactivation rate rather than deactivation by spontaneous emission alone. The other measurements of ϕ in the literature (Refs. 4, 14) are similar in nature to the present observations. Lifetime measurements indicated non exponential decay rates at pressures $P < 2\,\mu$, and homogeneous deactivation remained measurable at pressures where the mean free path for thermal molecules was larger than the radius of the container. The $A\,^2\Pi_u$ molecules thus appeared to be affected by an electric field, presumably caused by the differential diffusion of ions and electrons. The effect was also apparent at pressures $P > 2\,\mu$ where the $A\,^2\Pi_u$ deactivation coefficient displayed electron current and energy dependence.

Cross-sections were thus necessarily determined by measurements of emission rate and ϕ, at pressures $P > 2\,\mu$ where ϕ was a well defined quantity. The computation of the cross-sections consequently required a measure of the natural lifetime (τ) of the $A\,^2\Pi_u$ state. However τ is not a well-determined quantity for the same reason that the cross-sections cannot be measured directly. The cross-sections given here are lower limit estimates based on the extrapolated lifetime measurements by Ref. (14) ($\tau_{(2)} = 6.6\,\mu$ sec). The estimated total cross-section is 1.2×10^{-16} cm^2 at $E = 100$ eV. This is a factor of 2–5 larger than the previous cross-section estimates. The measured relative population rates of the $A\,^2\Pi_u$ state correlate very well with the theoretical rates for the $A\,^2\Pi_u - X\,^1\Sigma_g^+$ transition. Time of flight measurements by Ref. (15) ($\tau \approx 12\,\mu$sec), which should be free of the difficulties encountered here, are too large to be compatible with the present work since the estimated $A\,^2\Pi_u$ cross-section would then equal the well established total ionization cross-section. However, there is some evidence to support the measurements of Ref. (14) as being not too far from the real values; the relative lifetimes of the $A\,^2\Pi_u$ levels are in good agreement with the values determined from the relative transition probabilities (Part I). The excitation functions of the $A\,^2\Pi_u$ levels are linear in E from threshold to about $E = 30$ eV. The shape of the function, corrected by the lifetime measurements, has been determined up to $E = 100$ eV.

Accurate measurements of the total ionization cross-section near threshold (Refs. 16, 17), from which the N_2^+M cross-section can be estimated, are in good agreement with the present work.

The photoionization measurements by Ref. (18) are also consistent with the cross-section obtained here since both indicate relative production rates $(QM/Q1N) \approx 6$.

REFERENCES

1. J. W. McConkey and F. R. Simpson, *J. Phys. B Proc. phys. Soc.* **2,** 923 (1969).
2. P. N. Stanton and R. M. St. John, *J. Opt. Soc. Am.* **59,** 252 (1969).
3. B. N. Srivastava and I. M. Mirza, *Can. J. Phys.* **47,** 475 (1969).
4. F. R. Simpson and J. W. McConkey, *Planet. Space Sci.* **17,** 1941 (1969).
5. D. J. Burns, F. R. Simpson, J. W. McConkey, *J. Phys. B.* **2,** 52 (1969).
6. J. D. Jobe, F. A. Sharpton, and R. M. St. John, *J. Opt. Soc. Am.* **57,** 106 (1967).
7. I. P. Zapesochnyi and V. V. Skubenich, *Opt. Spectrosc.* **21,** 83 (1966).
8. V. V. Skubenich and I. P. Zapesochnyi, *5th Int. Conf. on the Physics of Electronic and Atomic Collisions,* (1967).
9. M. Jeunehomme, *J. chem. Phys.* **45,** 1805 (1966).
10. D. E. Shemansky and A. L. Broadfoot, *JQSRT* **11,** 1385 (1971).
11. N. Thompson and S. E. Williams, *Proc. R. Soc.* **A147,** 583 (1934).
12. O. Oldenberg, *Planet. Space Sci.* **1,** 40 (1959).
13. W. F. Sheridan, O. Oldenberg, and N. P. Carleton, *Atomic Collision Processes* (Ed. M. R. C. McDowell). North-Holland, Amsterdam (1964).
14. R. O'Neil and G. Davidson, Air Force Cambridge Research Laboratories Tech. Rep. AFCRL-67-0277 (1967).
15. M. Hollstein, D. C. Lorents, J. R. Peterson, and J. R. Sheridan, *Can. J. Chem.* **47,** 1858 (1969).
16. R. E. Fox, *J. chem. Phys.* **35,** 1379 (1961).
17. R. Rapp and P. Englander-Golden, *J. chem. Phys.* **43,** 1464 (1965).
18. R. I. Schoen, *J. chem. Phys.* **40,** 1830 (1964).
19. D. E. Shemansky and A. Vallance-Jones, *Planet. Space Sci.* **16,** 1115 (1968).
20. D. E. Shemansky and N. P. Carleton, *J. chem. Phys.* **51,** 682 (1969).
21. E. Zipf and W. Borst, *Phys. Rev.* **1,** 834 (1970).
22. R. G. Bennett and F. W. Dalby, *J. chem. Phys.* **31,** 434 (1959).
23. J. E. Hesser, *J. chem. Phys.* **48,** 2518 (1968).
24. L. V. Wallace and R. W. Nicholls, *J. atm. terr. Phys.* **7,** 101 (1955).
25. D. C. Tyte, *Proc. phys. Soc.* **80,** 1347 (1962).
26. W. Benesch, J. T. Vanderslice, S. G. Tilford, and P. G. Wilkinson, Astrophys. *J.* **143,** 236 (1966); **144,** 408 (1966).
27. A. L. Broadfoot and D. M. Hunten, *Can. J. Phys.* **42,** 1212 (1964).
28. D. M. Hunten and G. G. Shepherd, *J. atm. terr. Phys.* **6,** 64 (1955).
29. J. F. M. Aarts, F. J. de Heer and L. Vriens, *6th Int. Conf. on the Physics of Electronic and Atomic Collisions* (1969).
30. T. Wentink Jr., E. P. Marram, L. Isaacson, Air Force Weapons Laboratory, Tech. Rep. AFWL-TR-67-6 (1967).
31. R. W. Nicholls, *J. Res. Natn. Bur. Stand.* **A65,** 451 (1961).
32. L. J. Kieffer and G. H. Dunn, *Rev. Mod. Phys.* **38,** 1 (1966).
33. J. T. Tate and P. T. Smith, *Phys. Rev.* **39,** 270 (1932).
34. I. M. Campbell and B. A. Thrush, *Proc. R. Soc. (Lond.)* **A296,** 201 (1967).
35. A. J. Williams and J. P. Doering, *Planet. Space Sci.* **17,** 1527 (1969).
36. R. S. Freund, *J. chem. Phys.* **51,** 1979 (1969).
37. F. R. Gilmore, *JQSRT* **5,** 369 (1965).
38. D. E. Shemansky, *J. chem. Phys.* **51,** 689 (1969).
39. D. E. Shemansky and N. P. Carleton, *J. chem. Phys.* **51,** 682 (1969).
40. A. L. Broadfoot and S. P. Maran, *J. chem. Phys.* **51,** 678 (1969).
41. R. T. Brinkmann and S. Trajmar, *Ann. Geophys.* **26,** 201 (1970).
42. J. F. Noxon, *J. chem. Phys.* **36,** 926 (1962).
43. D. E. Shemansky, to be published.
44. M. P. Weinreb and G. G. Mannella, *J. chem. Phys.* **51,** 4973 (1969).
45. K. D. Bayes and G. B. Kistiakowsky, *J. chem. Phys.* **32,** 992 (1960).
46. R. J. Oldman and H. P. Broida, *J. chem. Phys.* **51,** 2254 (1969).
47. M. Jeunehomme and A. B. F. Duncan, *J. chem. Phys.* **41,** 1692 (1964).
48. R. G. Fowler, C. C. Lin, R. M. St. John, Air Force Weapons Laboratory, Tech. Report AFWL-TR-66-132 (1967).
49. B. A. Thrush, *J. chem. Phys.* **47,** 3691 (1967).
50. J. B. Hasted, *Physics of Atomic Collisions.* Butterworths (1964).
51. W. H. Kasner, *Phys. Rev.* **164,** 194 (1967).
52. M. J. Seaton, *Phys. Rev.* **113,** 814 (1959).
53. E. C. Zipf, *J. chem. Phys.* **38,** 2034 (1963).

APPENDIX

Deactivation probability of N_2A molecules by reaction 8

Due to lack of direct measurements of the deactivation rates of N_2A molecules the deactivation probability of reaction 8 must be estimated through the use of the diffusion equation and the observed pressure dependence of the ratios (IB_v/IB_4). The estimation of the magnitude k_8 is necessarily crude, because of the complex shape of the collision chamber and the fact that the surfaces are not efficient deactivators of the $A\ ^3\Sigma_u^+$ state.

The deactivation probability (k_8) due to reaction with the surfaces of the collision chamber can be described by the equation,

$$k_8 = \alpha(\bar{v}/\bar{L}) \tag{A1}$$

where $\bar{v}$ is the mean velocity. $\bar{L}$ is the transport length, and α is the efficiency factor (cf. HASTED[50]).

In the low pressure region where homogeneous collisions can be neglected, the transport length has no dependence on the diffusion coefficient and is determined only by the geometry of the chamber and the electron beam. The diameter of the electron beam is small compared to the dimensions of the chamber, and can be neglected. A crude approximation to the shape of the chamber is a truncated cylinder with a height (H) roughly twice the radius (R). The transport length ($\bar{L}$) in the low pressure case is therefore a little larger than the value it would have for a sphere. We estimate the transport coefficient to be roughly 1.4, and thus $\bar{L}_0 = R \times 1.4 = 2.6$ cm. This then represents the minimum transport length for deactivation at the surfaces. The maximum deactivation probability is then $k_8(\text{max.}) \approx 2 \times 10^4\ \text{sec}^{-1}$, from Equation A1.

The complete equation for $\bar{L}$ at any pressure includes the transport length due to homogeneous collisions, and is approximated by the following:

$$\bar{L} = \bar{L}_0 + [N_2]\bar{L}' \tag{A2}$$

where $\bar{L}' = \bar{v}/K^2D'$, K is the reciprocal of the diffusion length, and the constant D' is the diffusion coefficient-pressure product.

The rather sudden change in pressure dependence of (IB_v/IB_4) below $P = 3\mu$, and the near independence of $[N_2]$ at higher pressures, demands that k_8 must decrease rapidly beginning at pressures below $3\ \mu$. In order to obtain a good fit to the observations the transport length must double at $P = 1.6\ \mu$. This then determines K through equation A2; $K^2 = 0.19$. The value $D' = 153\ \text{cm}^2\ \text{sec}^{-1}$ Torr used for the calculation of K is due to the measurements by ZIPF.[53] The determination of K in turn determines the value of the effective radius of the chamber. If we assume fundamental mode diffusion to be dominant, K is given by (cf. Ref. 50),

$$K_1^2 = (2.40/R)^2 + (\pi/H)^2$$
$$\approx (4.0/R)^2$$

and $R = 9$ cm.

This value of R is much larger than the actual cylinder radius, $R = 1.9$ cm, and implies that the surfaces are not efficient deactivators of N_2A molecules. We now have a measure of the collision rate at the surface as a function of pressure.

The diffusion equation can be used to obtain a crude measure of the efficiency factor α, by determining the relative population densities at the surfaces, again assuming fundamental mode diffusion. This is given by the equation (cf. Ref. 50),

$$n(r, z)/n(0, 0) = J_0(2.40r/R) \cos z\pi/2R \tag{A3}$$

where (r), (z) are the radial and height distances, and $J_0(x)$ is the Bessel function of the first kind. We obtain an average value at the surfaces of $\bar{n}(r, z)/n(0, 0) = 0.84$, and

$$\alpha \approx 1 - \bar{n}(r, z)/n(0, 0) = 0.16.$$

The combination of Equations (A1, A2) then gives the following formula for k_8:

$$k_8 = 3.0 \times 10^3/(1 + 6.4 \times 10^2 P)\ \text{sec}^{-1} \tag{A4}$$

where P is in torr units.

This estimate must be compatible with observations of the spectral region where N_2 Vegard–Kaplan bands (VK) occur. The most likely prospect for observation in the present work is the N_2VK (1, 12) band at $\lambda = 3978$ Å. This part of the spectrum is clear of measureable features at any of the pressures at which spectra were obtained. The continuum in this region is also very weak, and we estimate the emission rate ratio $IVK(1,12)/I1N(0,0) < 10^{-3}$, for the case of a spectrum obtained at $E = 33$ eV and $P = 19\ \mu$. A lower limit to the value of k_8 can be calculated from this ratio in the following manner: The volume emission rate can be written,

$$IVK(1, 12) = F_e Q A_1 [N_2] A A_{1,12}/k_8, \tag{A5}$$

since the deactivation of the $A\ ^3\Sigma_u^+ v = 1$ level is controlled entirely by k_8 in this pressure region; the deactivation coefficient $k_3(1)$ is very small (cf. Ref. 43) and can be neglected, along with the probability for spontaneous emission. The cross-section QA_1 is determined entirely by cascade from the $B\ ^3\Pi_g$ state since direct excitation cross-sections of the lower levels of the $A\ ^3\Sigma_u^+$ state are negligible by comparison. We obtain the relationship

$$QA_1 = 2.7 QB_{3,1},$$

from the transition probability tables ($B\ ^3\Pi_g - A\ ^3\Sigma_u^+$) of Part I. The present estimate of $QB_{3,1}$ at 33 eV is 5.7×10^{-18} cm^2. Thus $QA_1 = 1.5 \times 10^{-17}$ cm^2. The effective transition probability of the $N_2VK(1, 12)$ band is $AA_{1,12} = 3.4 \times 10^{-2}$ sec^{-1} (Ref. 38). The volume emission rate,

$$I1N(0, 0) = F_e Q1N_{0,0}[N_2], \tag{A6}$$

where $(Q1N_{0,0}) = 8.0 \times 10^{-18}$ cm^2 at 33 eV. Thus we have the ratio, from Equations (A5, A6),

$$IVK(1, 12)/I1N(0, 0) = QA_1 A_{1,12}/(Q1N_{0,0})k_8 < 10^{-3}, = 6.6 \times 10^{-2}/k_8 < 10^{-3},$$

and $k_8 > 0.7 \times 10^2$ sec^{-1}. At $P = 19\ \mu$, Equation A4 gives $k_8 = 2.3 \times 10^2$ sec^{-1}.